Electronic Supplementary Material (ESI) for Chemical Science.

Electronic Supplementary Information

Rare Earth Dialkyl Cations and Monoalkyl Dications supported by a Rigid Neutral Pincer Ligand: Synthesis and Ethylene Polymerization

Aathith Vasanthakumar, Jeffrey S. Price and David J. H. Emslie*

Department of Chemistry, McMaster University, 1280 Main St. West, Hamilton, Ontario, L8S 4M1, Canada. Fax: (905)-522-2509; Tel: (905)-525-9140 x 23307.

E-mail: emslied@mcmaster.ca. Website: https://emsliegroup.mcmaster.ca/

Contents

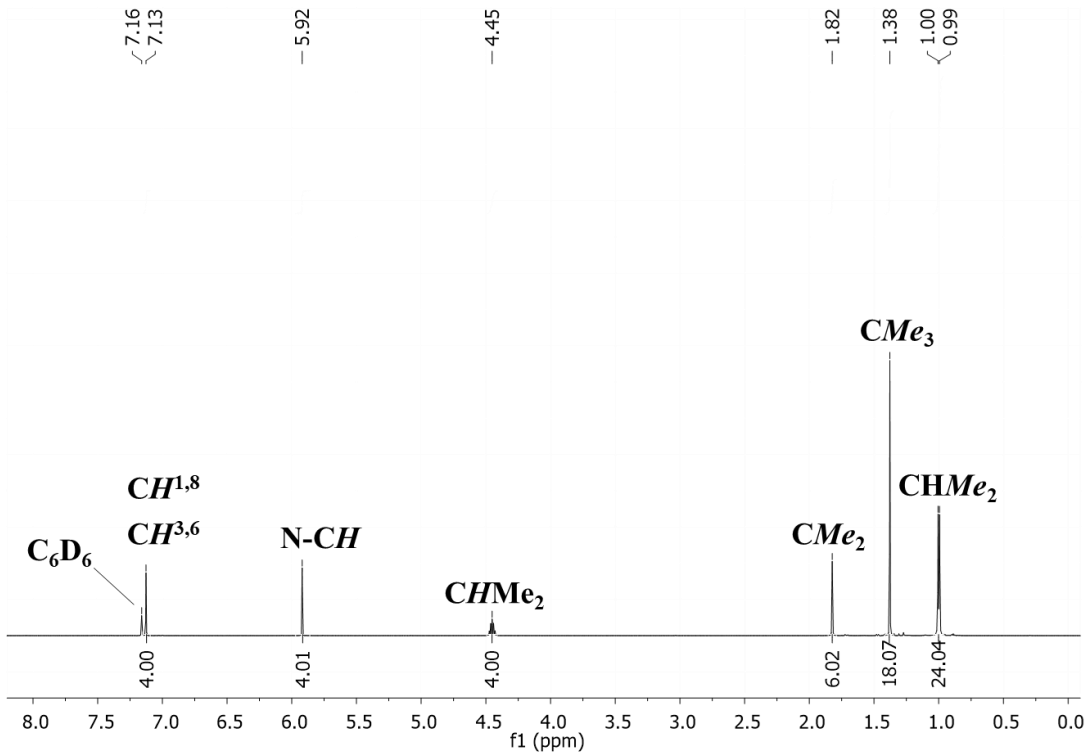

Figure S1. ^{1}H NMR spectrum of the XII_2 ligand (600 MHz, C_6D_6).

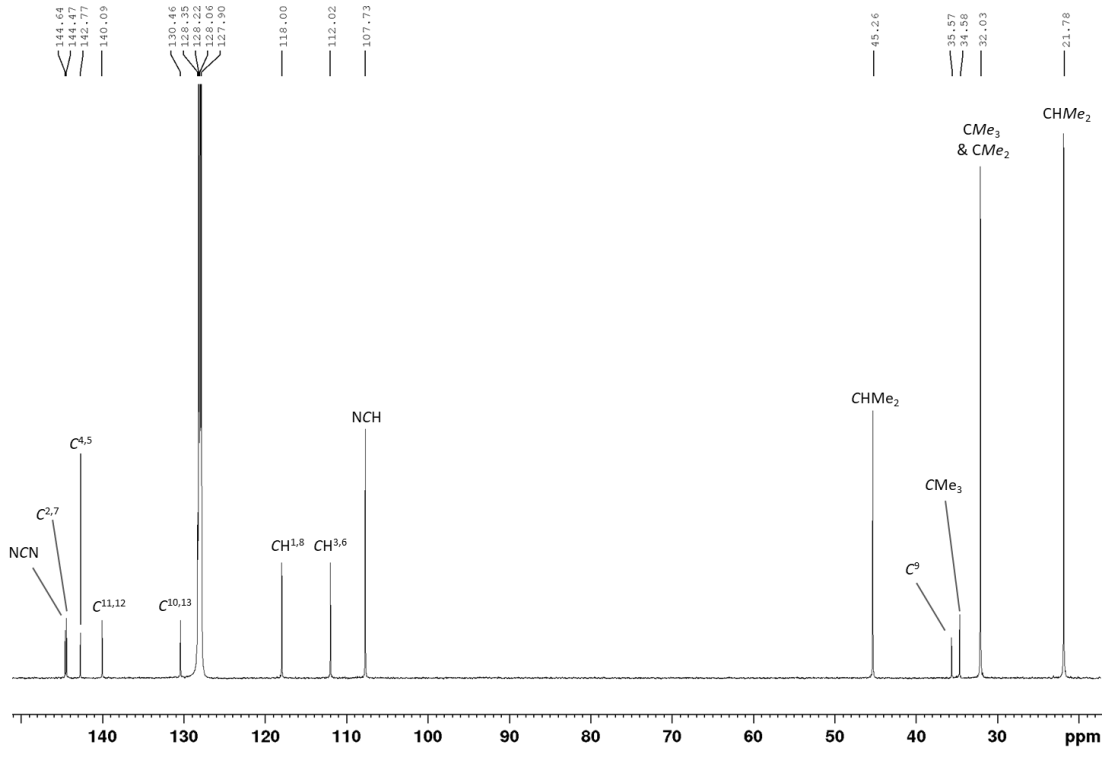

Figure S2. $^{13}C\{^{1}H\}$ NMR spectrum of the XII_2 ligand (151 MHz, C_6D_6).

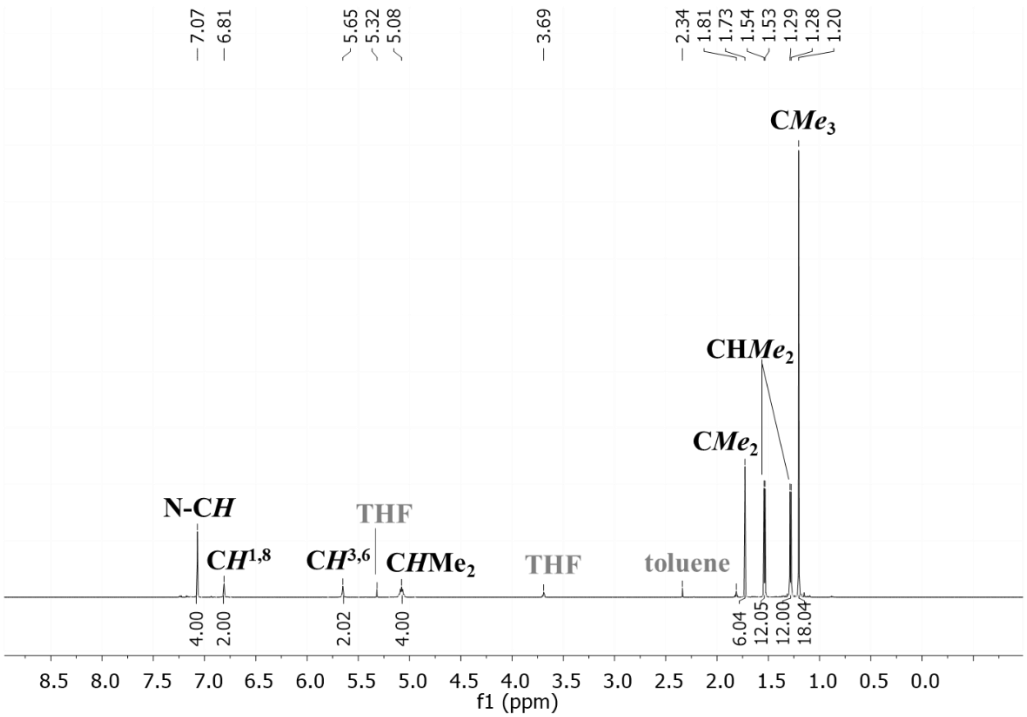

Figure S3. ^{1}H NMR spectrum of $[(XII_2)YCl_3]$ (**1**) (600 MHz, CD_2Cl_2).

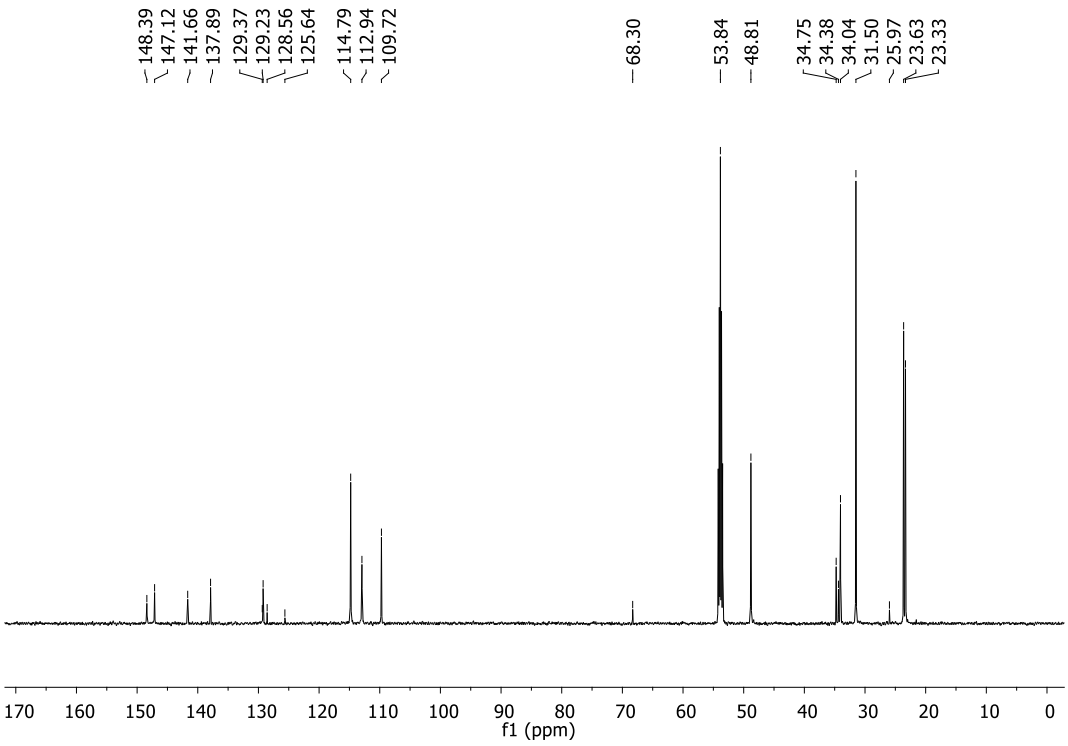

Figure S4. $^{13}C\{^{1}H\}$ NMR spectrum of $[(XII_2)YCl_3]$ (**1**) (151 MHz, CD_2Cl_2). See Figures S5 and S6 for expanded regions of the spectrum with labelled peaks.

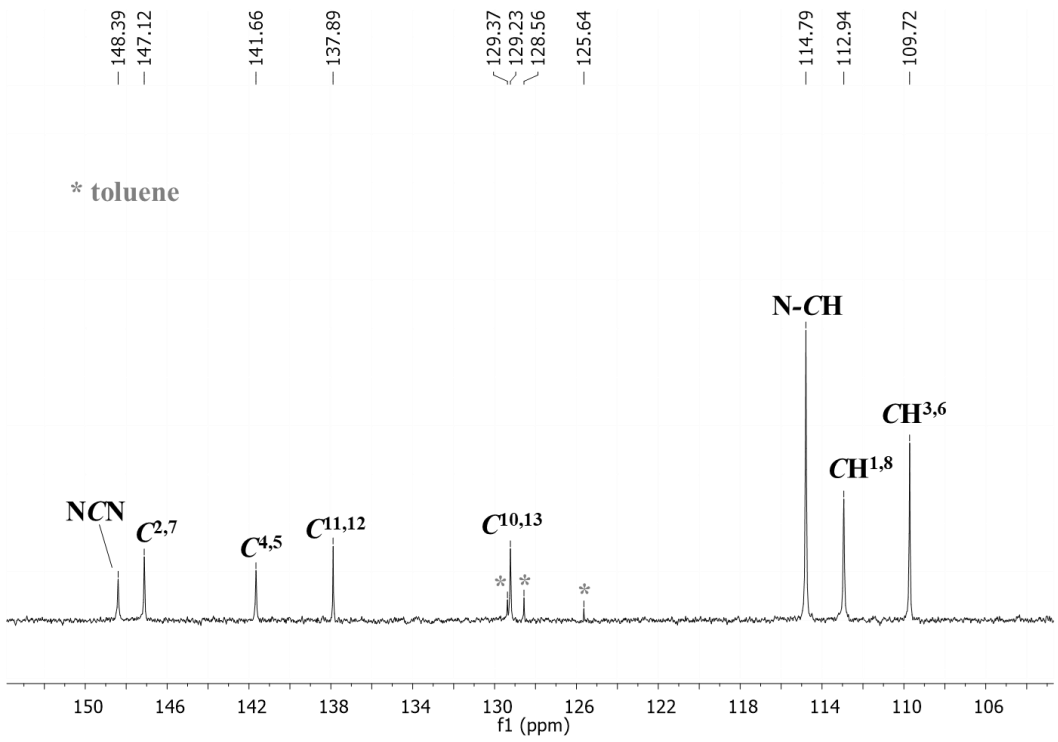

Figure S5. Expanded region of the $^{13}C\{^{1}H\}$ NMR spectrum of $[(XII_2)YCl_3]$ (**1**) (151 MHz, CD_2Cl_2).

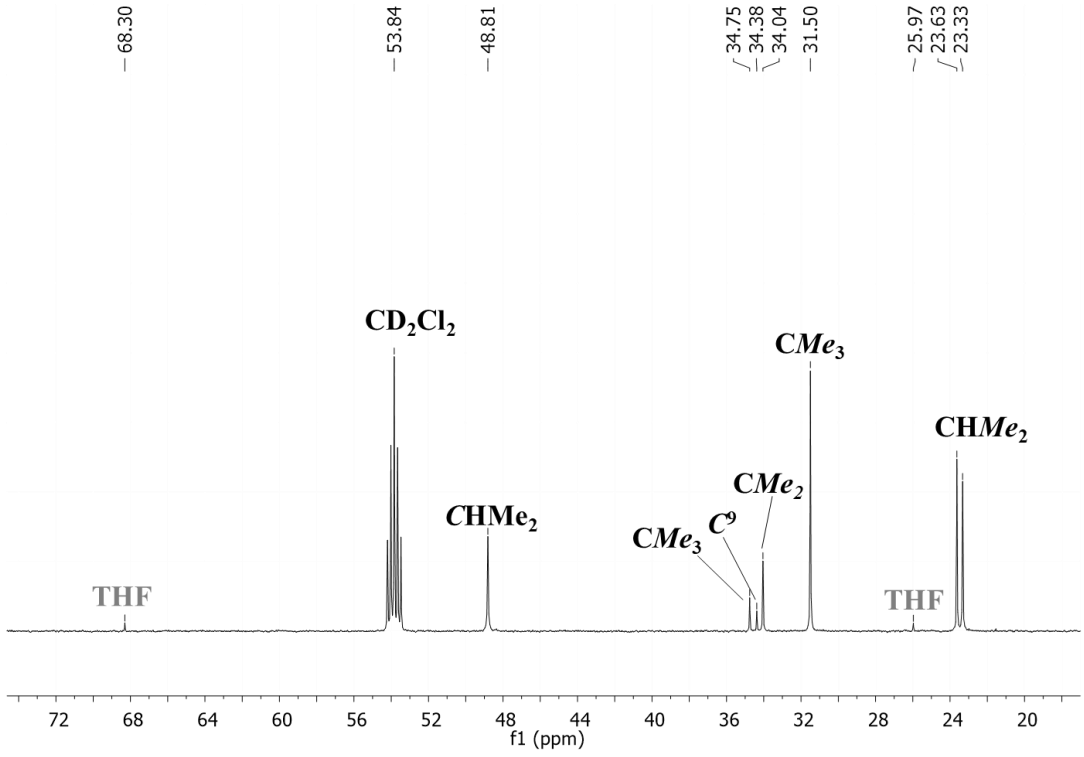

Figure S6. Expanded region of the $^{13}C\{^{1}H\}$ NMR spectrum of $[(XII_2)YCl_3]$ (**1**) (151 MHz, CD_2Cl_2).

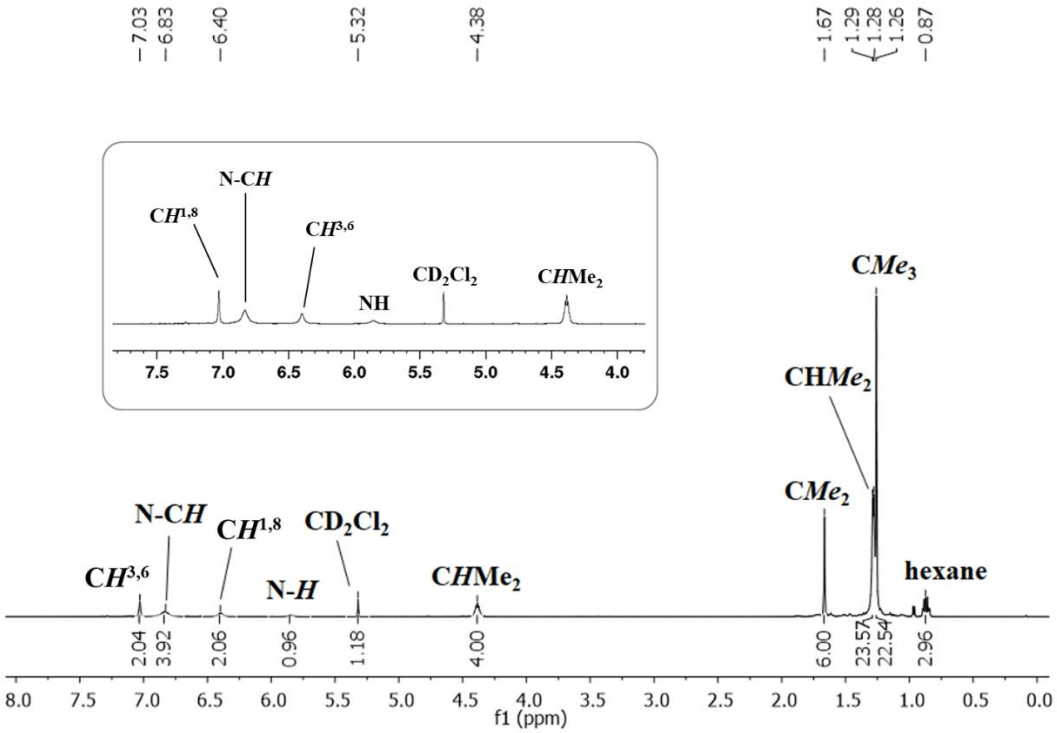

Figure S7. ^{1}H NMR spectrum of [H(XII$_2$)][B(C$_6$F$_5$)$_4$]·0.5 hexane (600 MHz, CD_2Cl_2).

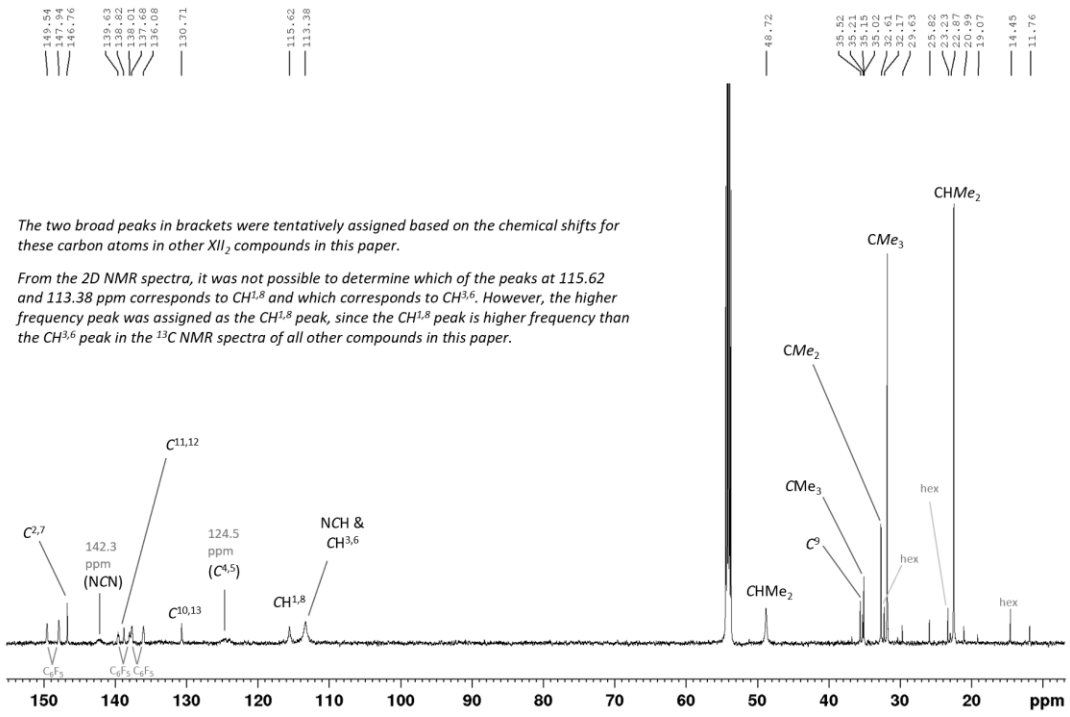

Figure S8. ^{13}C{^{1}H} NMR spectrum of [H(XII$_2$)][B(C$_6$F$_5$)$_4$]·0.5 hexane (151 MHz, CD_2Cl_2).

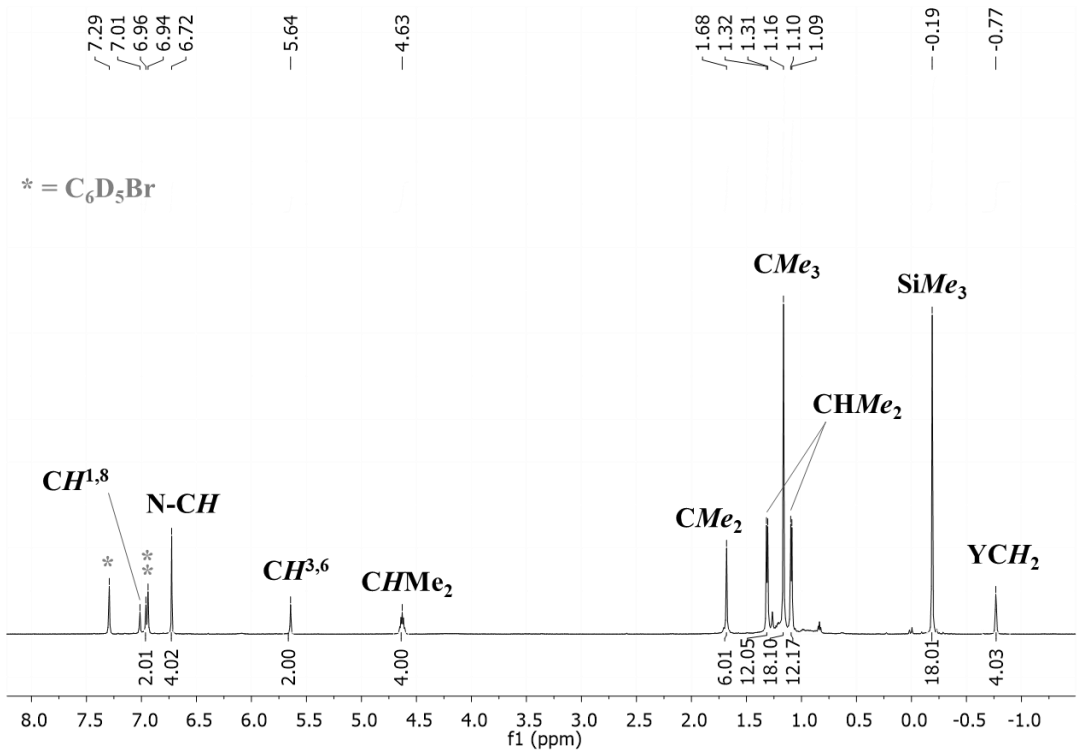

Figure S9. ^{1}H NMR spectrum of $[(XII_2)Y(CH_2SiMe_3)_2][B(C_6F_5)_4]$ (**2**) (600 MHz, C_6D_5Br).

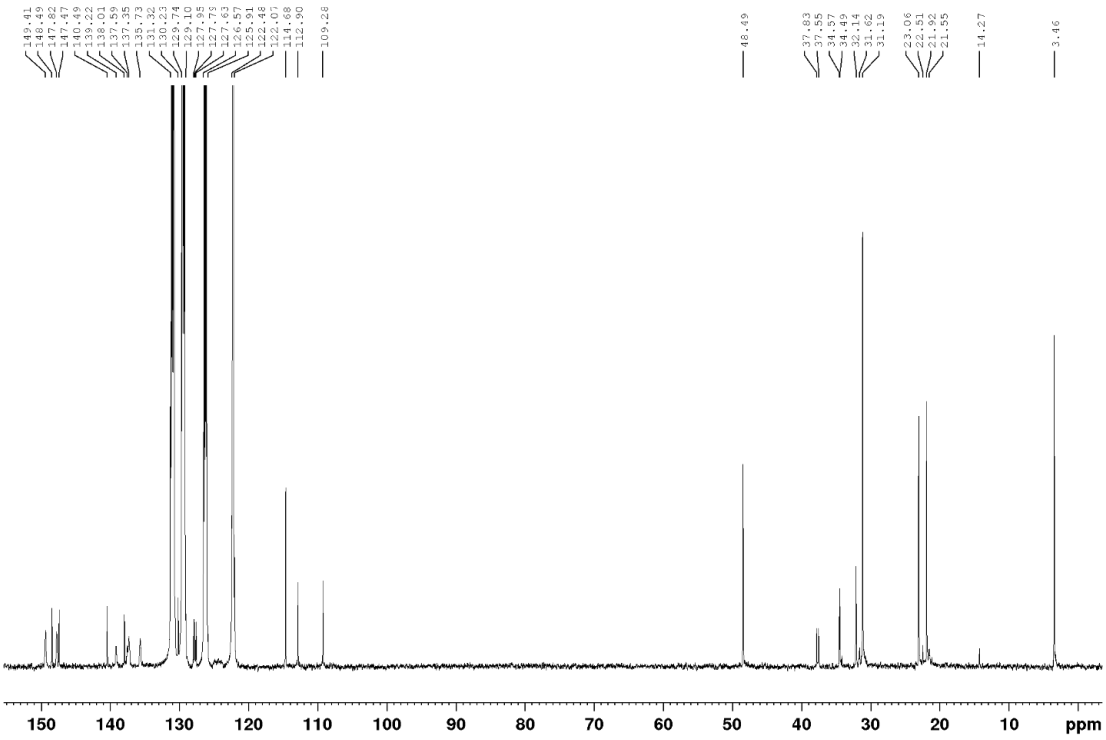

Figure S10. $^{13}C\{^{1}H\}$ NMR spectrum of $[(XII_2)Y(CH_2SiMe_3)_2][B(C_6F_5)_4]$ (**2**) (151 MHz, C_6D_5Br). See Figures S11 and S12 for expanded regions of the spectrum with labelled peaks.

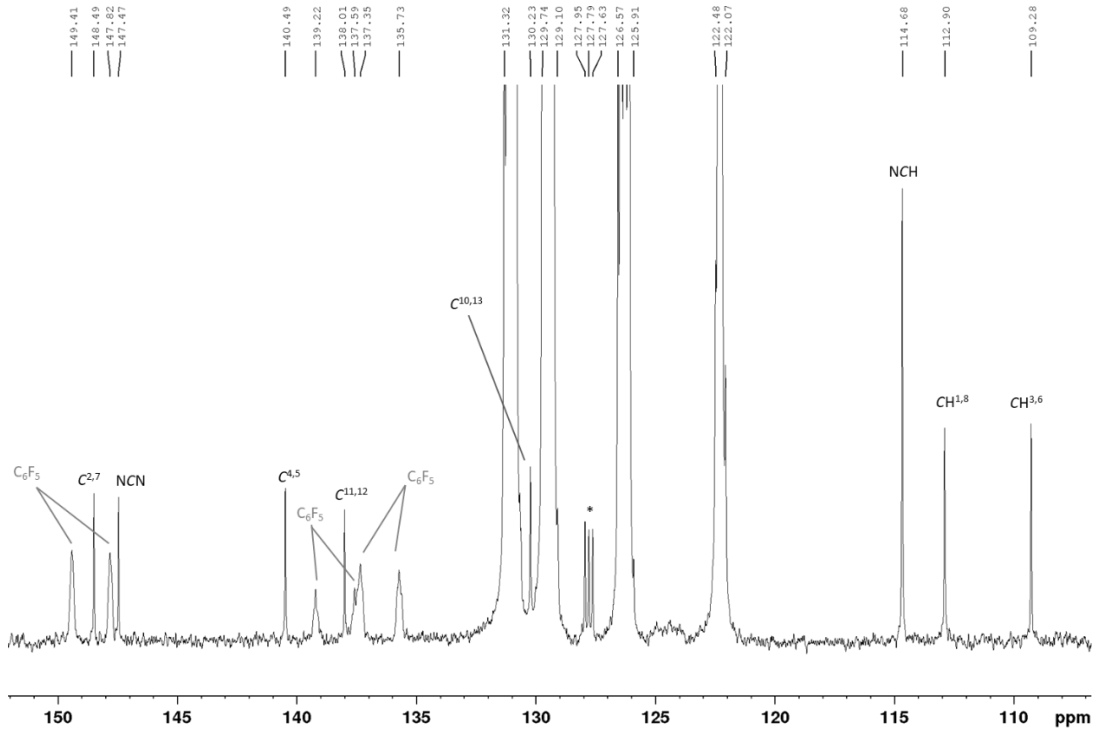

Figure S11. Expanded region of the $^{13}C\{^1H\}$ NMR spectrum of $[(XII_2)Y(CH_2SiMe_3)_2][B(C_6F_5)_4]$ (**2**) (151 MHz, C_6D_5Br).

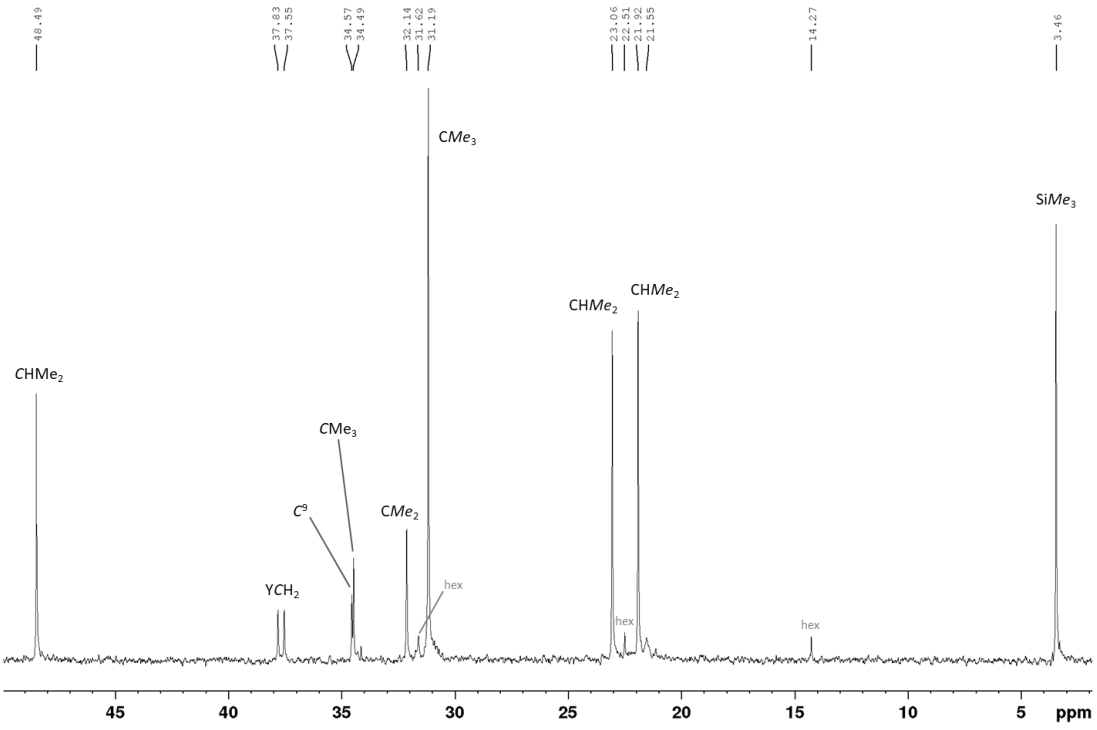

Figure S12. Expanded region of the $^{13}C\{^1H\}$ NMR spectrum of $[(XII_2)Y(CH_2SiMe_3)_2][B(C_6F_5)_4]$ (**2**) (151 MHz, C_6D_5Br).

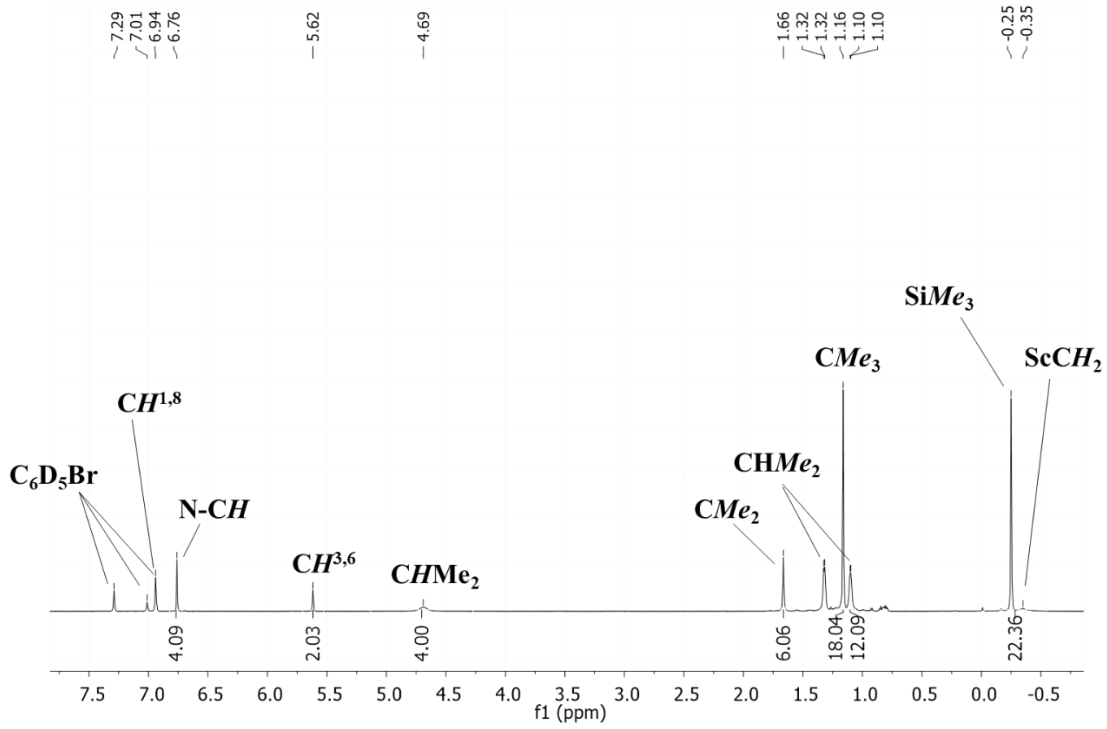

Figure S13. ^{1}H NMR spectrum of $[(XII_2)Sc(CH_2SiMe_3)_2][B(C_6F_5)_4]$ (**3**) (600 MHz, C_6D_5Br).

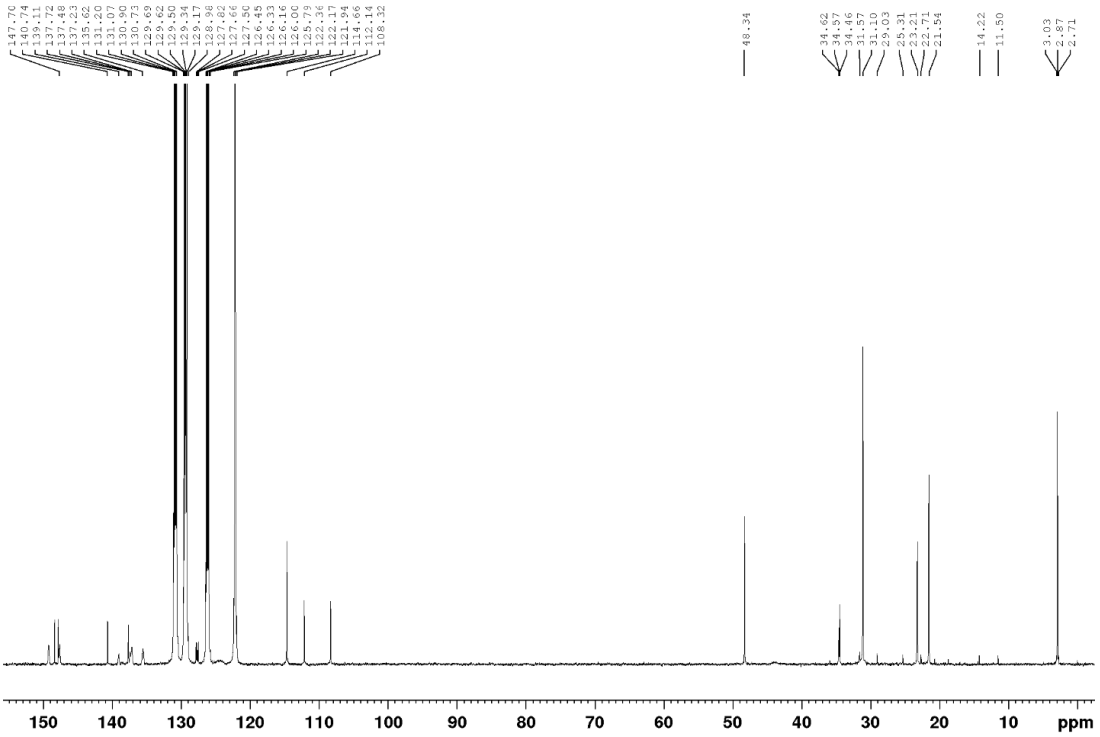

Figure S14. $^{13}C\{^{1}H\}$ NMR spectrum of $[(XII_2)Sc(CH_2SiMe_3)_2][B(C_6F_5)_4]$ (**3**) (151 MHz, C_6D_5Br). See Figures S15 and S16 for expanded regions of the spectrum with labelled peaks.

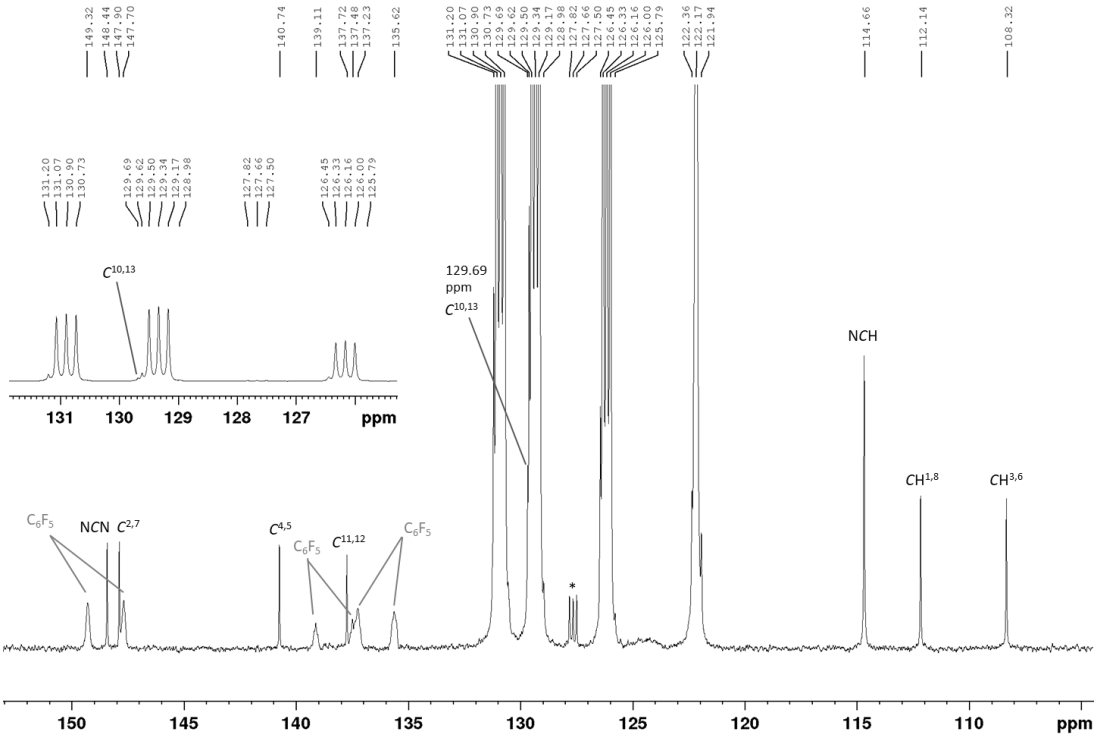

Figure S15. Expanded region of the $^{13}C\{^1H\}$ NMR spectrum of $[(XII_2)Sc(CH_2SiMe_3)_2][B(C_6F_5)_4]$ (**3**) (151 MHz, C_6D_5Br).

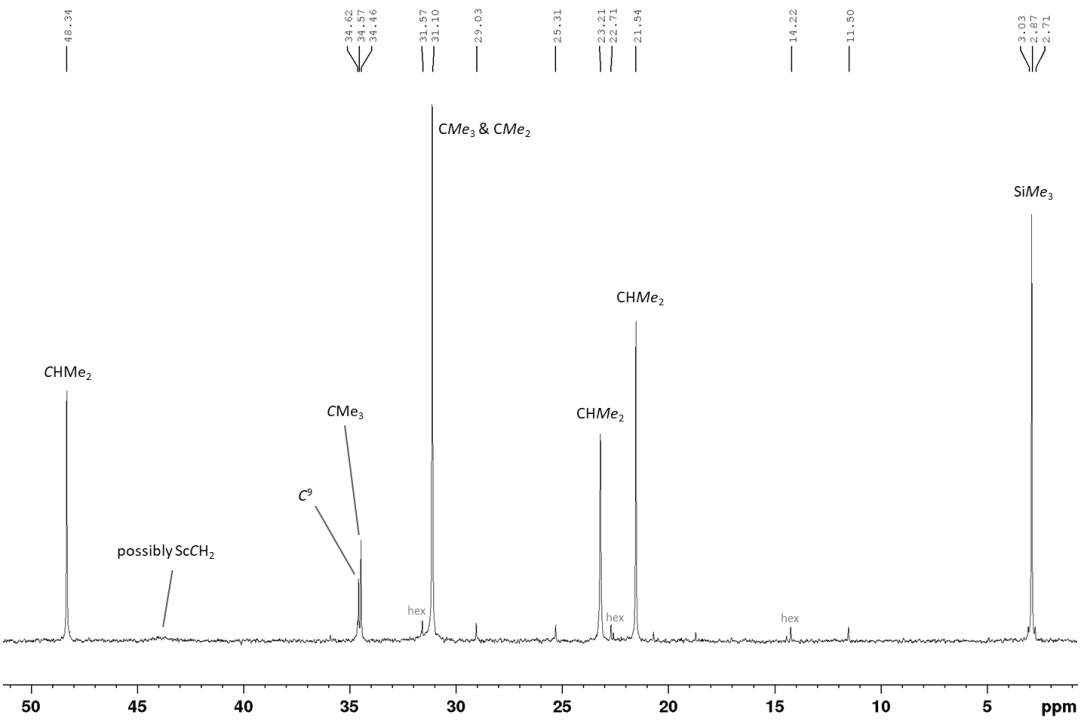

Figure S16. Expanded region of the $^{13}C\{^1H\}$ NMR spectrum of $[(XII_2)Sc(CH_2SiMe_3)_2][B(C_6F_5)_4]$ (**3**) (151 MHz, C_6D_5Br).

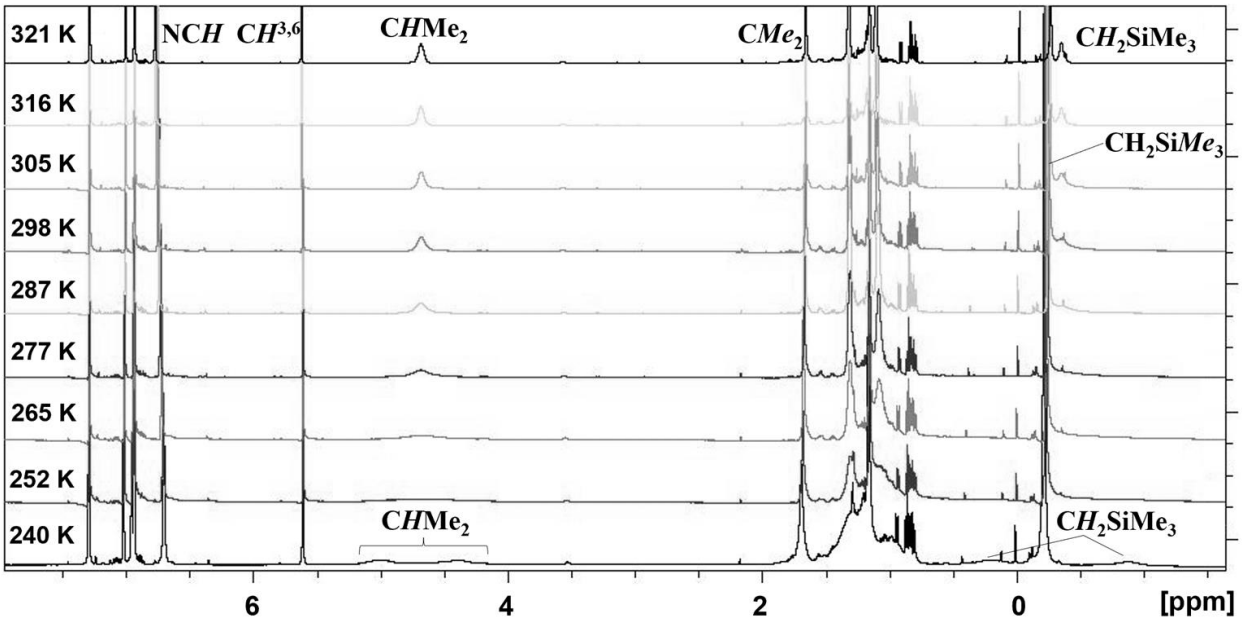

Figure S17. Variable temperature ^{1}H NMR spectra of $[(XII_2)Sc(CH_2SiMe_3)_2][B(C_6F_5)_4]$ (**3**) (500 MHz, C_6D_5Br).

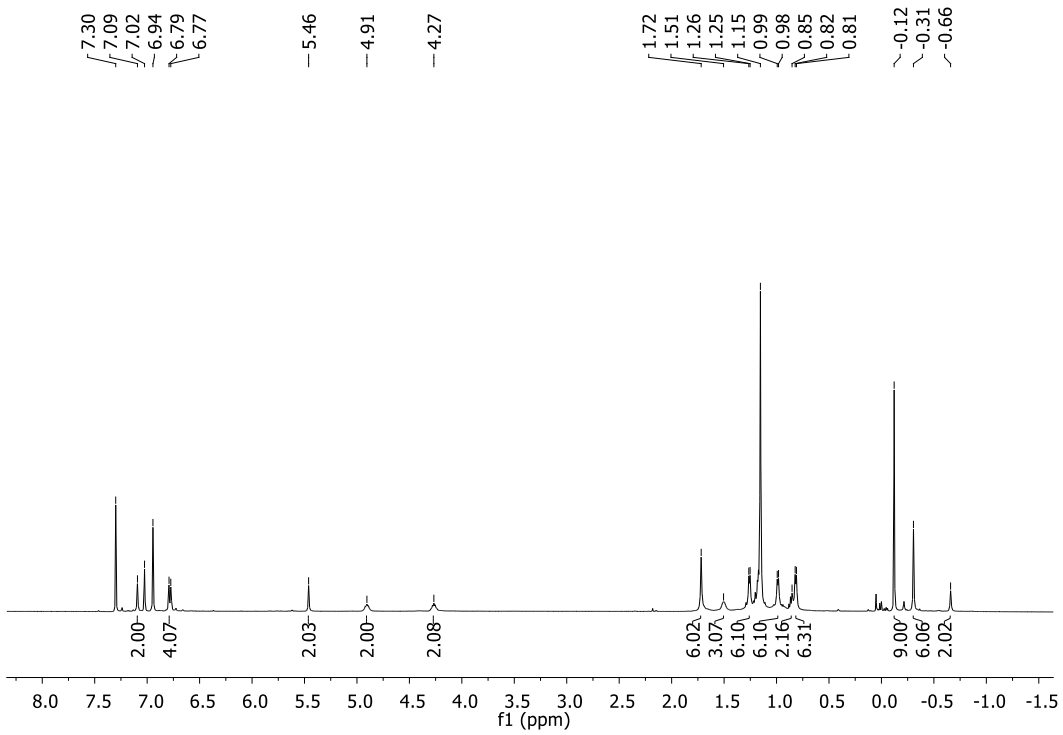

Figure S18. Low temperature ^{1}H NMR spectrum of in situ generated $[(XII_2)Sc(CH_2SiMe_2CH_2SiMe_3)][MeB(C_6F_5)_3][B(C_6F_5)_4]$ (**4**) (500 MHz, 252K, C_6D_5Br). See Figures S19 and S20 for expanded regions of the spectrum with labelled peaks.

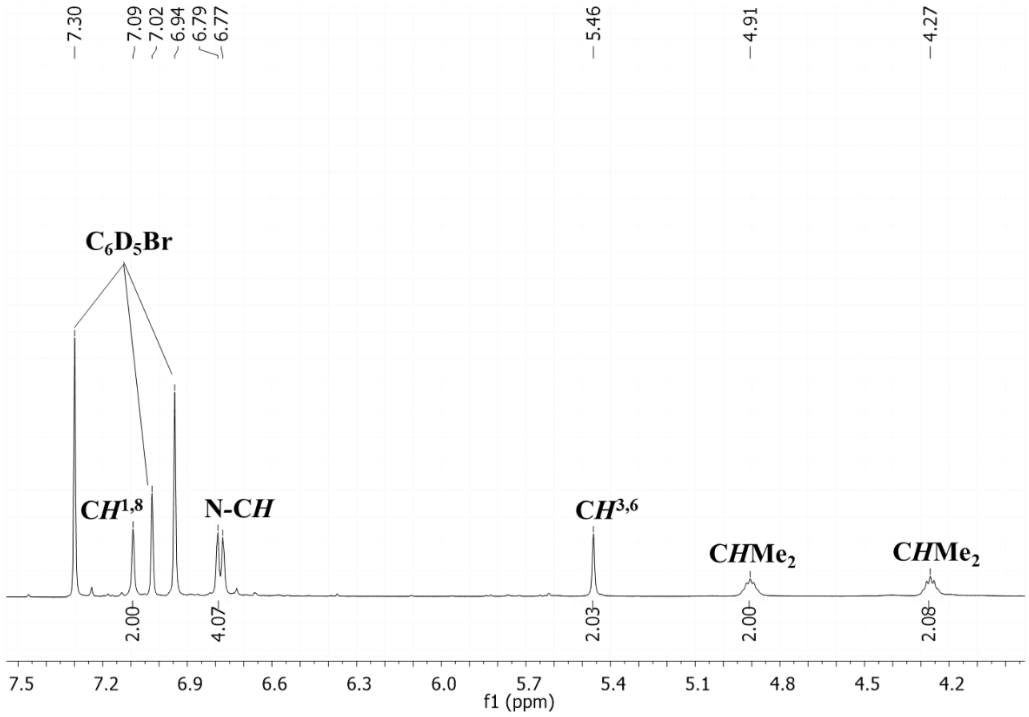

Figure S19. Expanded region of the low temperature ^{1}H NMR spectrum of in situ generated $[(XII_2)Sc(CH_2SiMe_2CH_2SiMe_3)][MeB(C_6F_5)_3][B(C_6F_5)_4]$ (**4**) (500 MHz, 252K, C_6D_5Br).

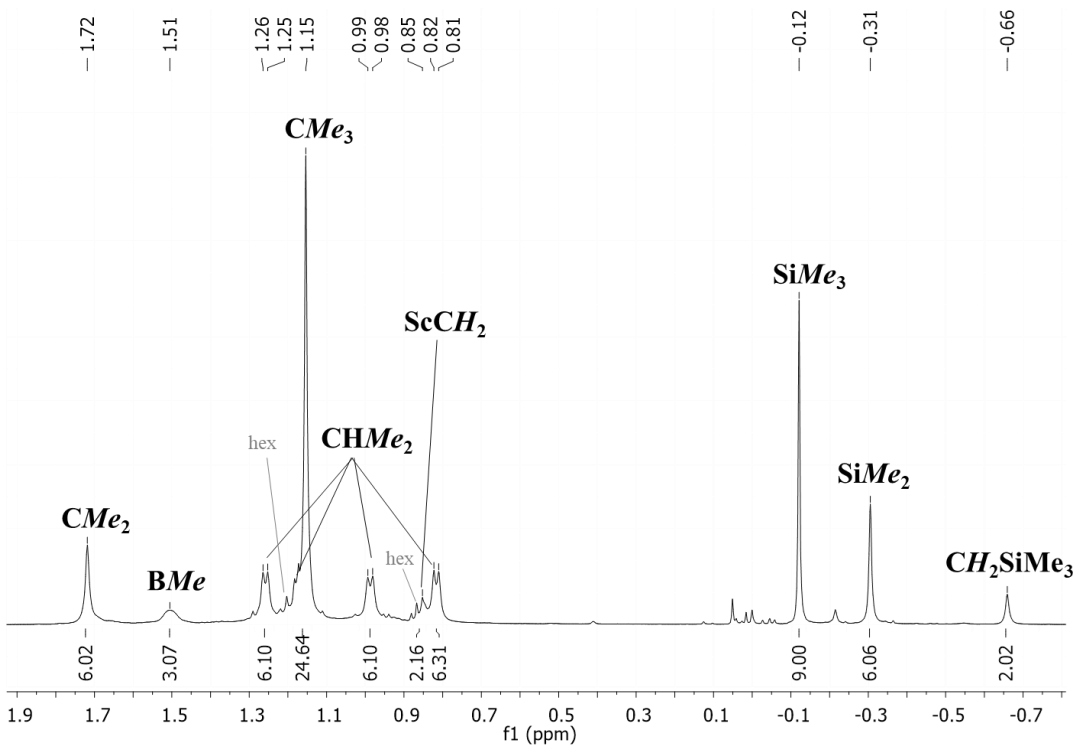

Figure S20. Expanded region of the low temperature ^{1}H NMR spectrum of in situ generated [(XII$_2$)Sc(CH$_2$SiMe$_2$CH$_2$SiMe$_3$)][MeB(C$_6$F$_5$)$_3$][B(C$_6$F$_5$)$_4$] (**4**) (500 MHz, 252K, C$_6$D$_5$Br).

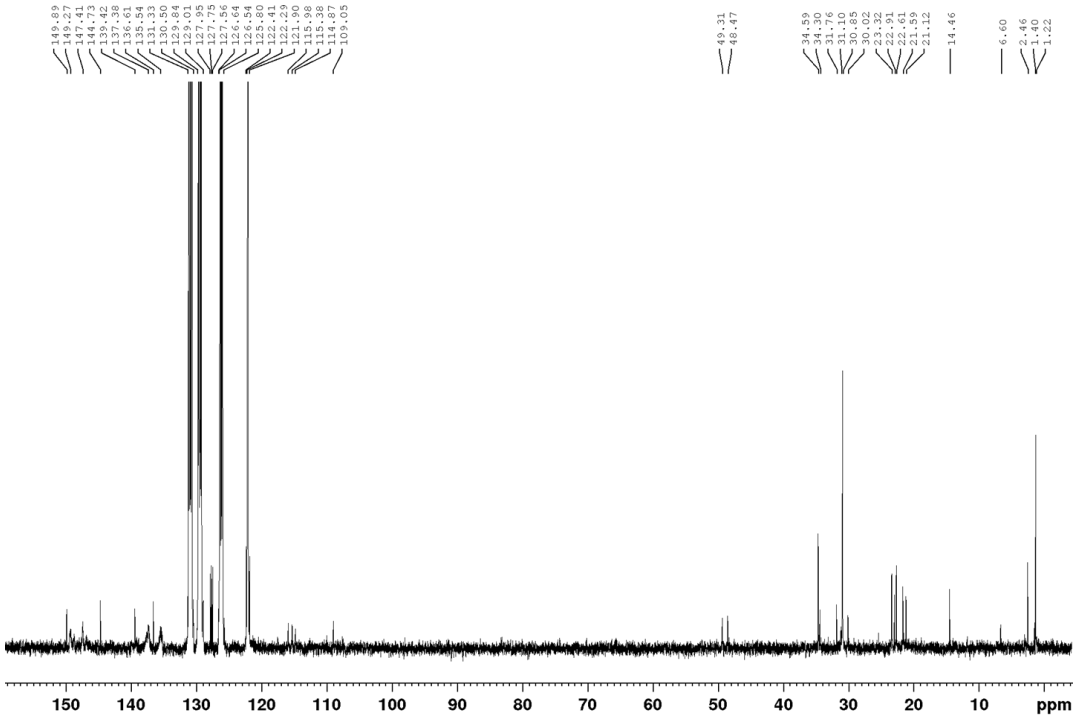

Figure S21. Low temperature ^{13}C{^{1}H} NMR spectrum of in situ generated [(XII$_2$)Sc(CH$_2$SiMe$_2$CH$_2$SiMe$_3$)][MeB(C$_6$F$_5$)$_3$][B(C$_6$F$_5$)$_4$] (**4**) (126 MHz, 252K, C$_6$D$_5$Br). See Figures S22 and S23 for expanded regions of the spectrum with labelled peaks.

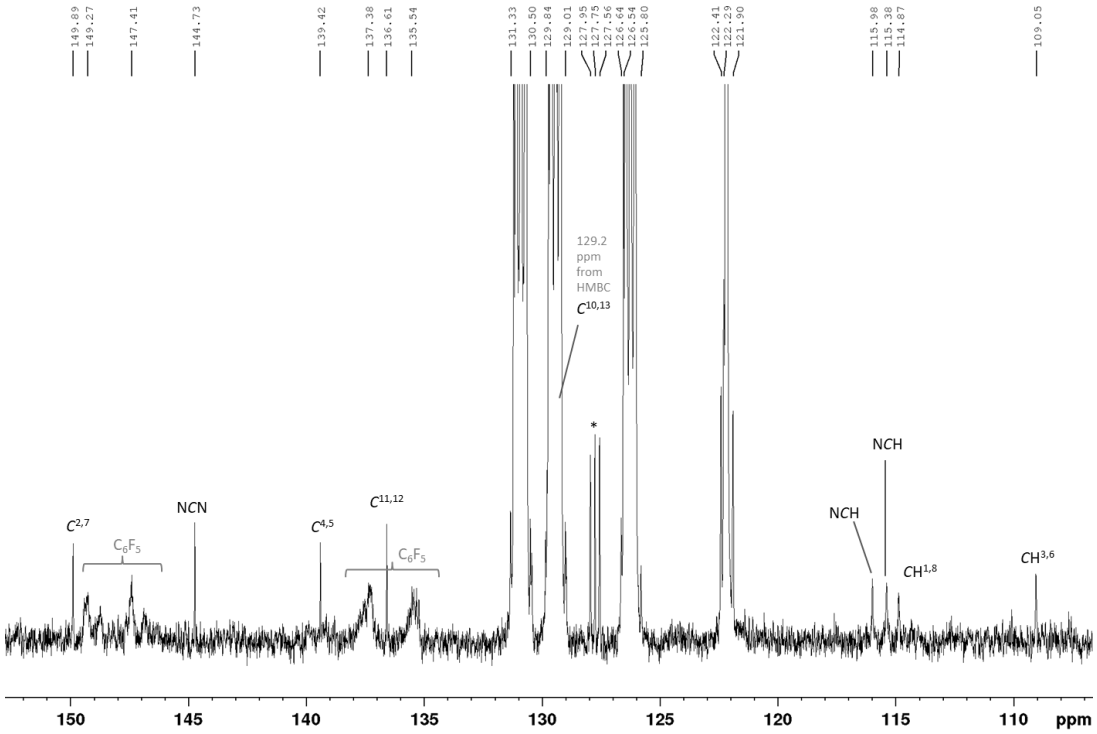

Figure S22. Expanded region of the low temperature $^{13}C\{^{1}H\}$ NMR spectrum of in situ generated $[(XII_2)Sc(CH_2SiMe_2CH_2SiMe_3)][MeB(C_6F_5)_3][B(C_6F_5)_4]$ (**4**) (126 MHz, 252K, C_6D_5Br).

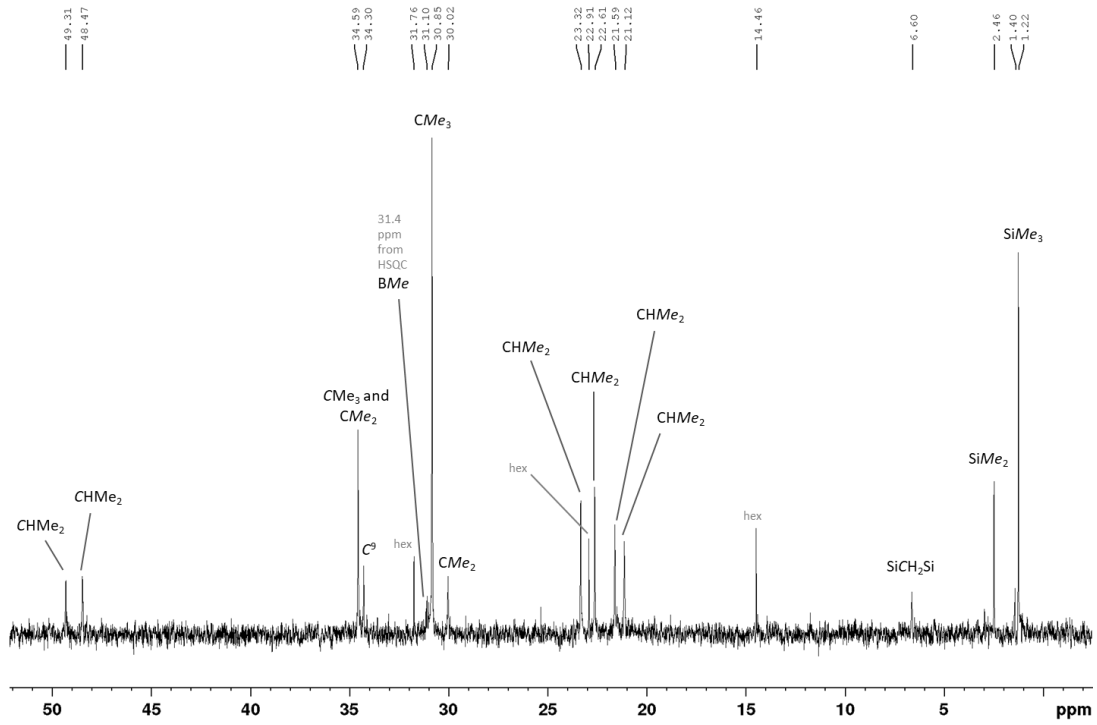

Figure S23. Expanded region of the low temperature $^{13}C\{^{1}H\}$ NMR spectrum of in situ generated $[(XII_2)Sc(CH_2SiMe_2CH_2SiMe_3)][MeB(C_6F_5)_3][B(C_6F_5)_4]$ (**4**) (126 MHz, 252K, C_6D_5Br).

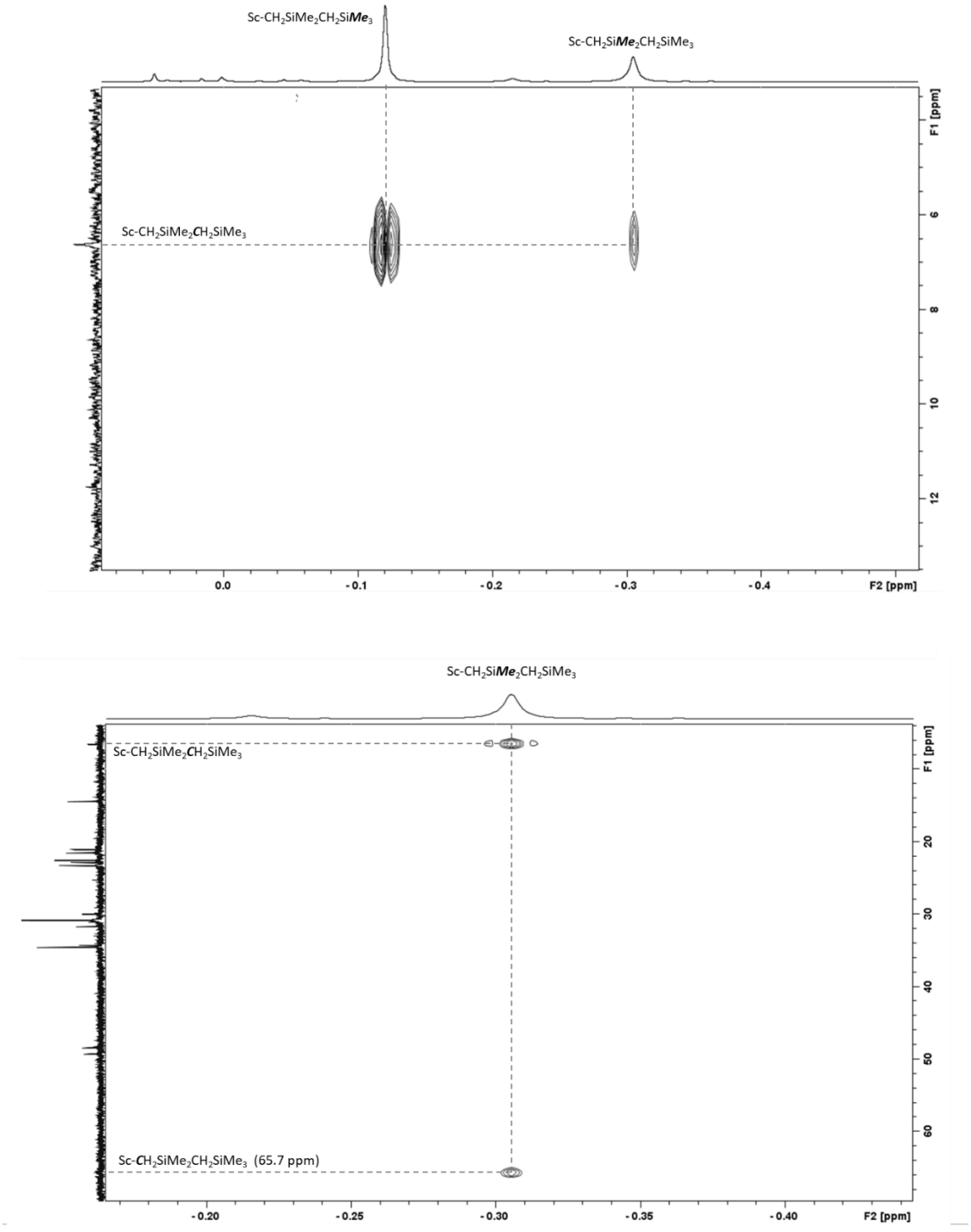

Figure S24. Regions of the low temperature ^{1}H-^{13}C HMBC NMR spectrum of in situ generated [(XII$_2$)Sc(CH$_2$SiMe$_2$CH$_2$SiMe$_3$)][MeB(C$_6$F$_5$)$_3$][B(C$_6$F$_5$)$_4$] (**4**) (500 MHz ^{1}H, 126 MHz ^{13}C, 252K, C$_6$D$_5$Br). The ^{1}H NMR spectrum is on the horizontal axis. The ^{13}C{^{1}H} NMR spectrum is on the vertical axis.

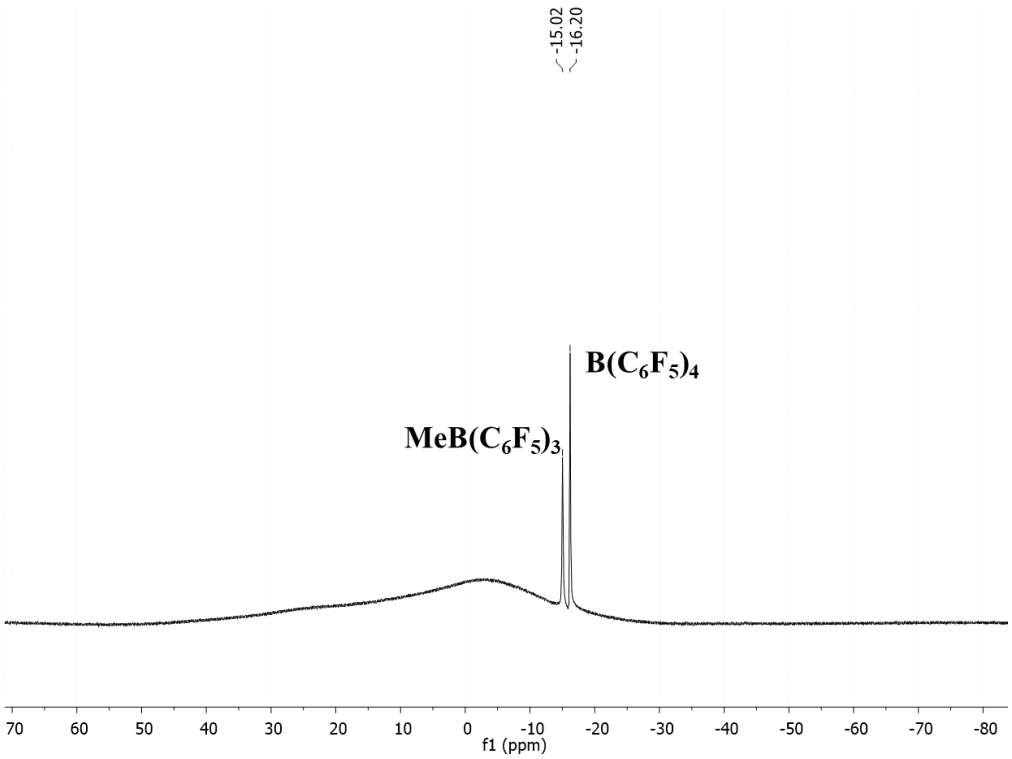

Figure S25. ^{11}B NMR Spectrum of in situ generated [(XII$_2$)Sc(CH$_2$SiMe$_2$CH$_2$SiMe$_3$)][MeB(C$_6$F$_5$)$_3$][B(C$_6$F$_5$)$_4$] (**4**) (161 MHz, 252K, C$_6$D$_5$Br).

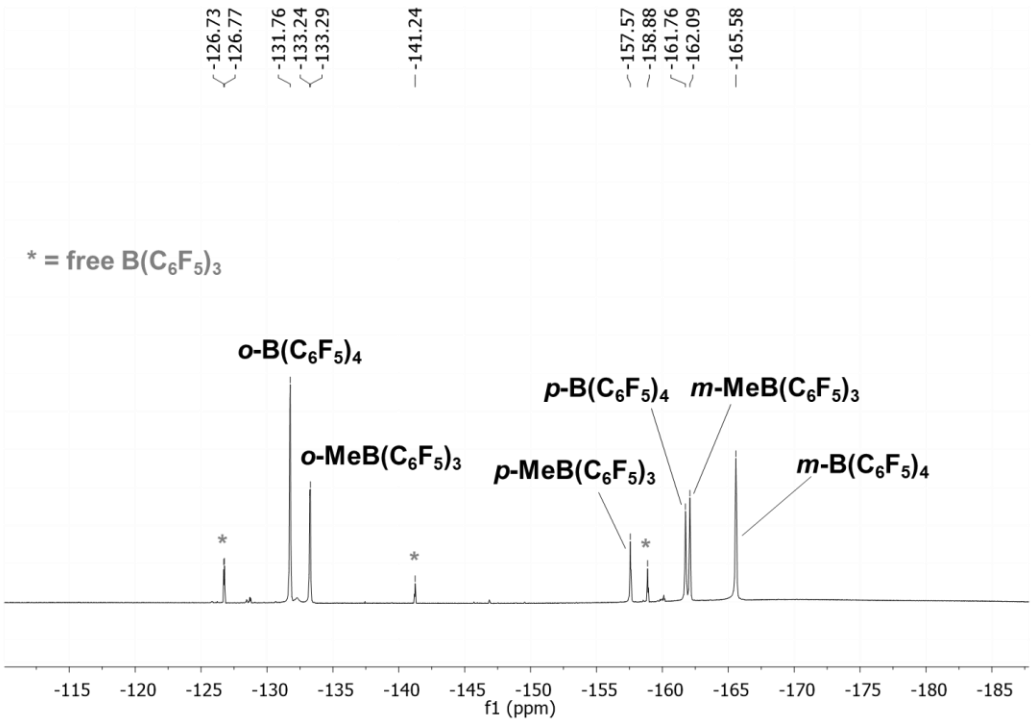

Figure S26. ^{19}F NMR Spectrum of in situ generated [(XII$_2$)Sc(CH$_2$SiMe$_2$CH$_2$SiMe$_3$)][MeB(C$_6$F$_5$)$_3$][B(C$_6$F$_5$)$_4$] (**4**) (471 MHz, 252K, C$_6$D$_5$Br).

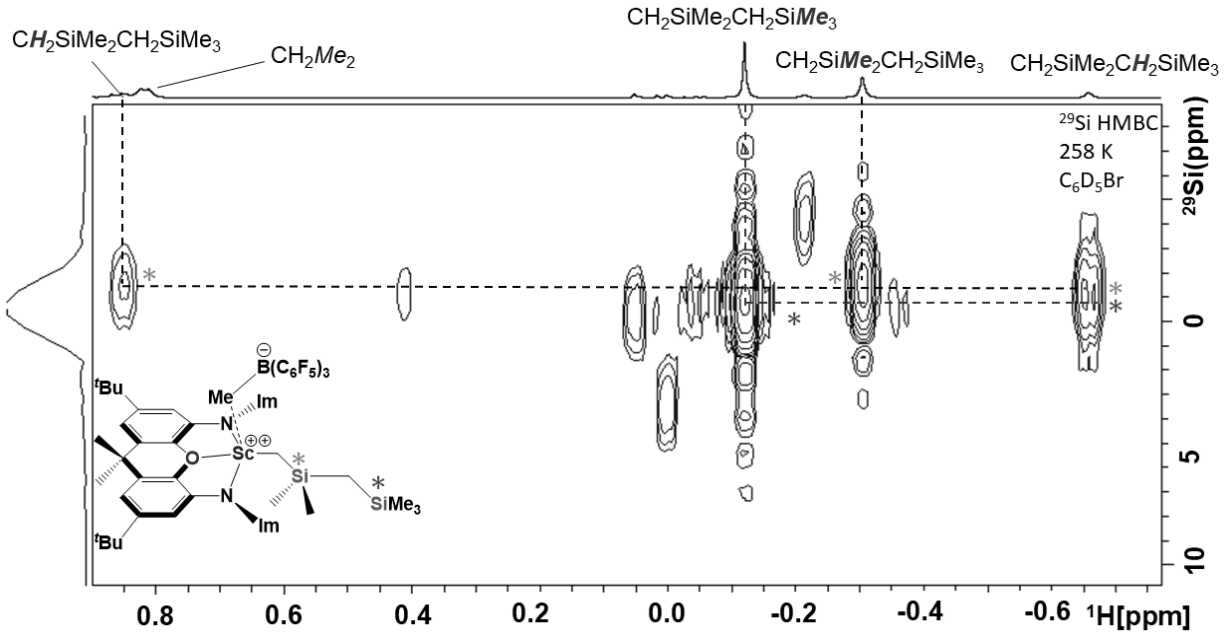

Figure S27. Region of the low temperature ^{1}H-^{29}Si HMBC NMR of $[(XII_2)Sc(CH_2SiMe_2CH_2SiMe_3)][MeB(C_6F_5)_3][B(C_6F_5)_4]$ (**4**) (500 MHz ^{1}H, 126 MHz ^{29}Si, 252K, C_6D_5Br). Note: the ^{29}Si NMR spectrum on the y-axis is an internal projection.

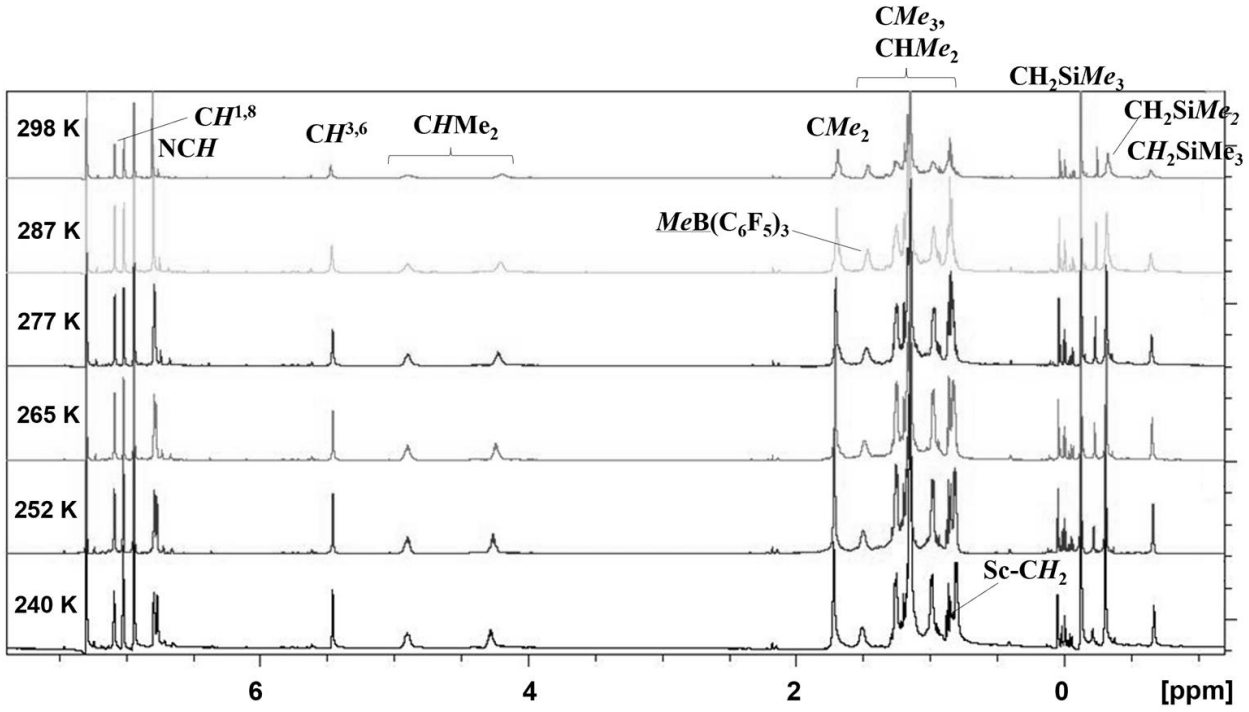

Figure S28. Variable temperature ^{1}H NMR spectra of in situ generated $[(XII_2)Sc(CH_2SiMe_2CH_2SiMe_3)][MeB(C_6F_5)_3][B(C_6F_5)_4]$ (**4**) (500 MHz, 252K, C_6D_5Br).

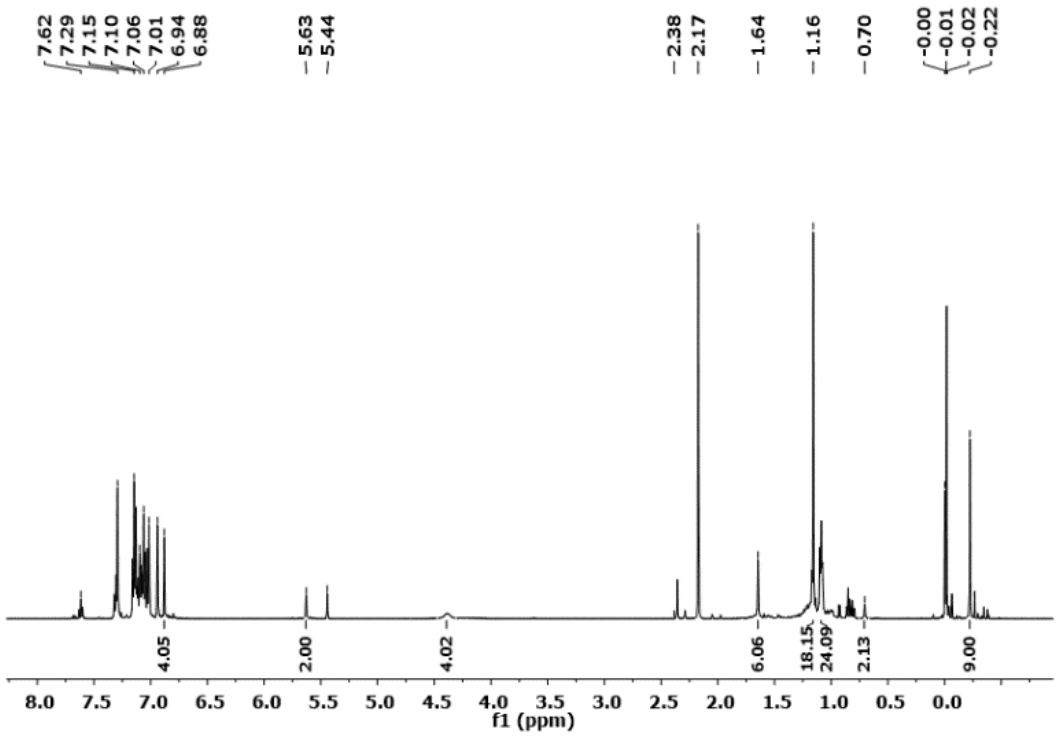

Figure S29. ^{1}H NMR spectrum of in situ generated [(XII$_2$)Sc(CH$_2$SiMe$_3$)(η^x-toluene)$_n$][B(C$_6$F$_5$)$_4$]$_2$ (**5**) in the presence of 5 equivalents of toluene (500 MHz, 298 K, C$_6$D$_5$Br). See Figures S30 and S31 for expanded regions of the spectrum with labelled peaks.

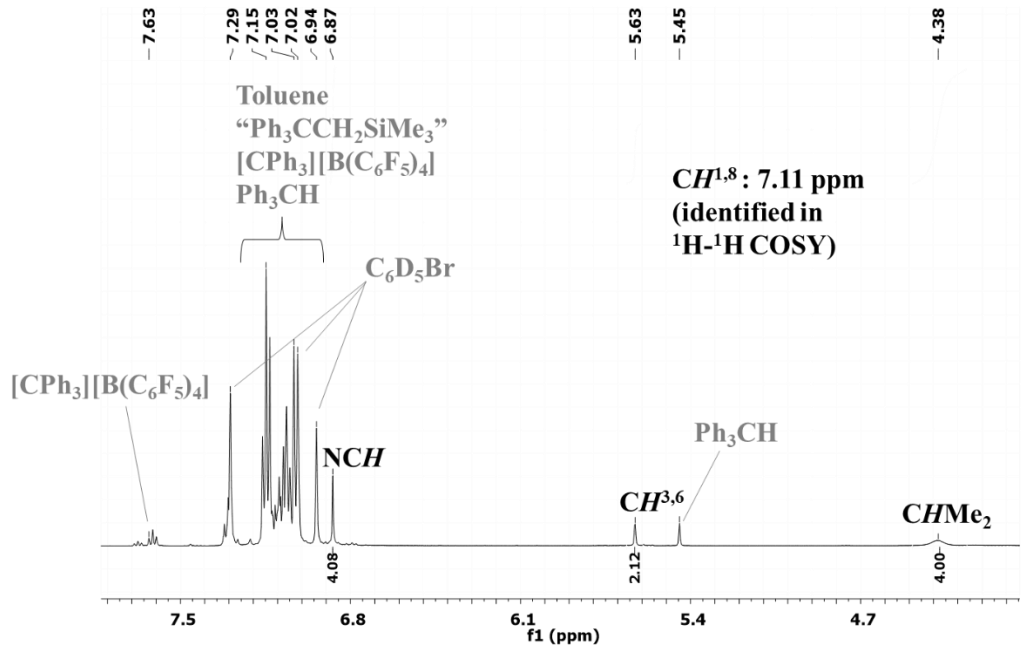

Figure S30. Region of the ^{1}H NMR spectrum of in situ generated [(XII$_2$)Sc(CH$_2$SiMe$_3$)(η^x-toluene)$_n$][B(C$_6$F$_5$)$_4$]$_2$ (**5**) in the presence of 5 equivalents of toluene (500 MHz, 298 K, C$_6$D$_5$Br).

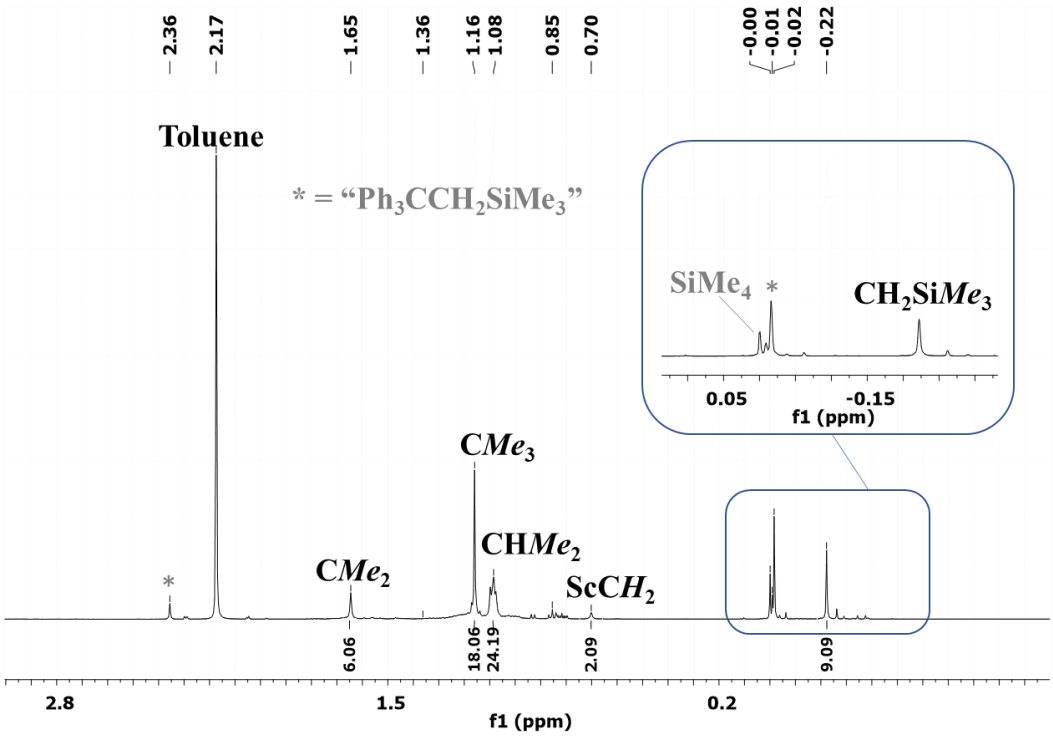

Figure S31. Region of the ^{1}H NMR spectrum of in situ generated [(XII$_2$)Sc(CH$_2$SiMe$_3$)(η^x-toluene)$_n$][B(C$_6$F$_5$)$_4$]$_2$ (**5**) in the presence of 5 equivalents of toluene (500 MHz, 298 K, C$_6$D$_5$Br).

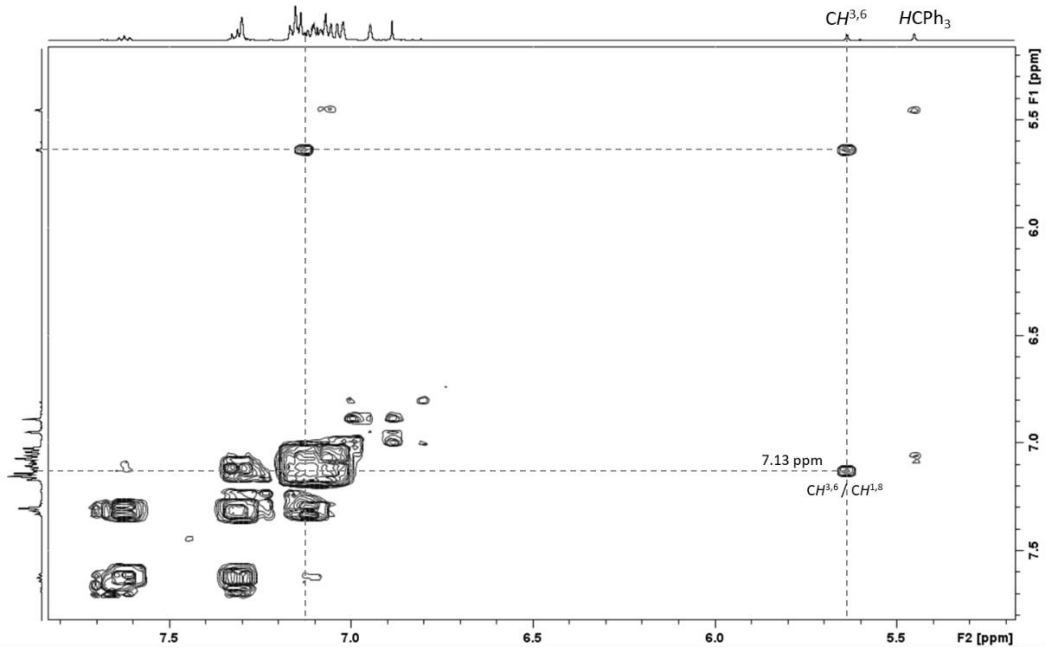

Figure S32. Region of the ^{1}H-^{1}H COSY NMR spectrum of in situ generated [(XII$_2$)Sc(CH$_2$SiMe$_3$)(η^x-toluene)$_n$][B(C$_6$F$_5$)$_4$]$_2$ (**5**) in the presence of 5 equivalents of toluene (500 MHz, 298 K, C$_6$D$_5$Br). This region of the spectrum enabled location of the C*H*^{1,8} proton signal.

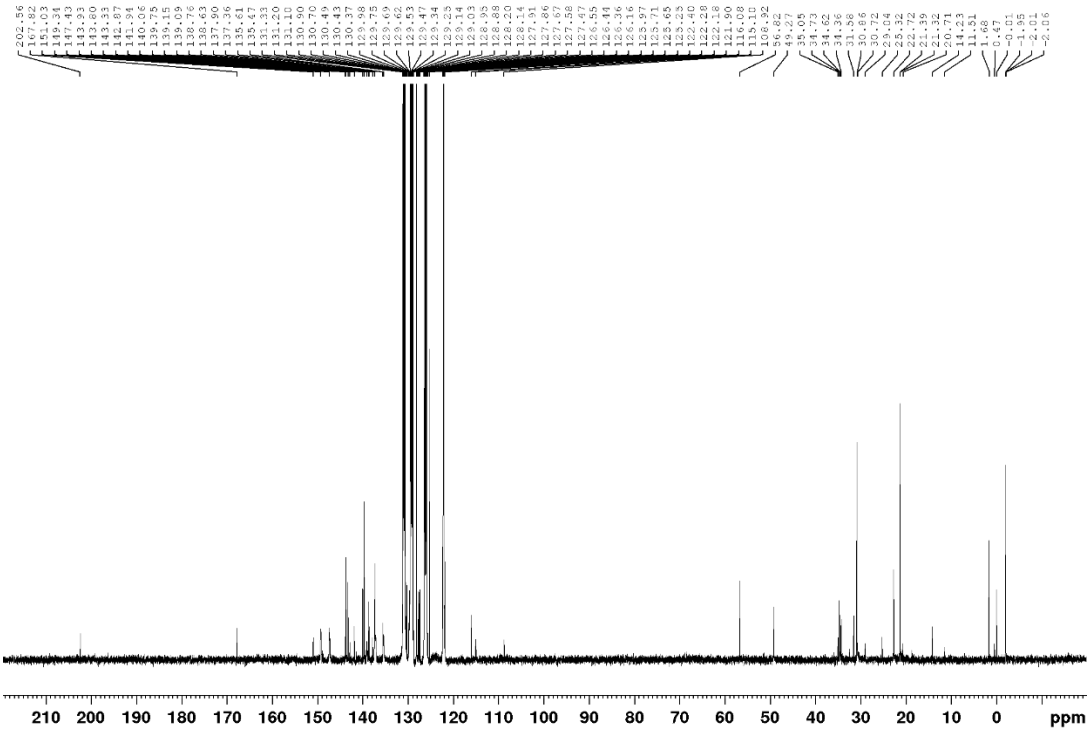

Figure S33. $^{13}C\{^{1}H\}$ NMR spectrum of in situ generated $[(XII_2)Sc(CH_2SiMe_3)(\eta^x\text{-toluene})_n][B(C_6F_5)_4]_2$ (**5**) in the presence of 5 equivalents of toluene (126 MHz, 298 K, C_6D_5Br). See Figures S34 and S35 for expanded regions of the spectrum with labelled peaks.

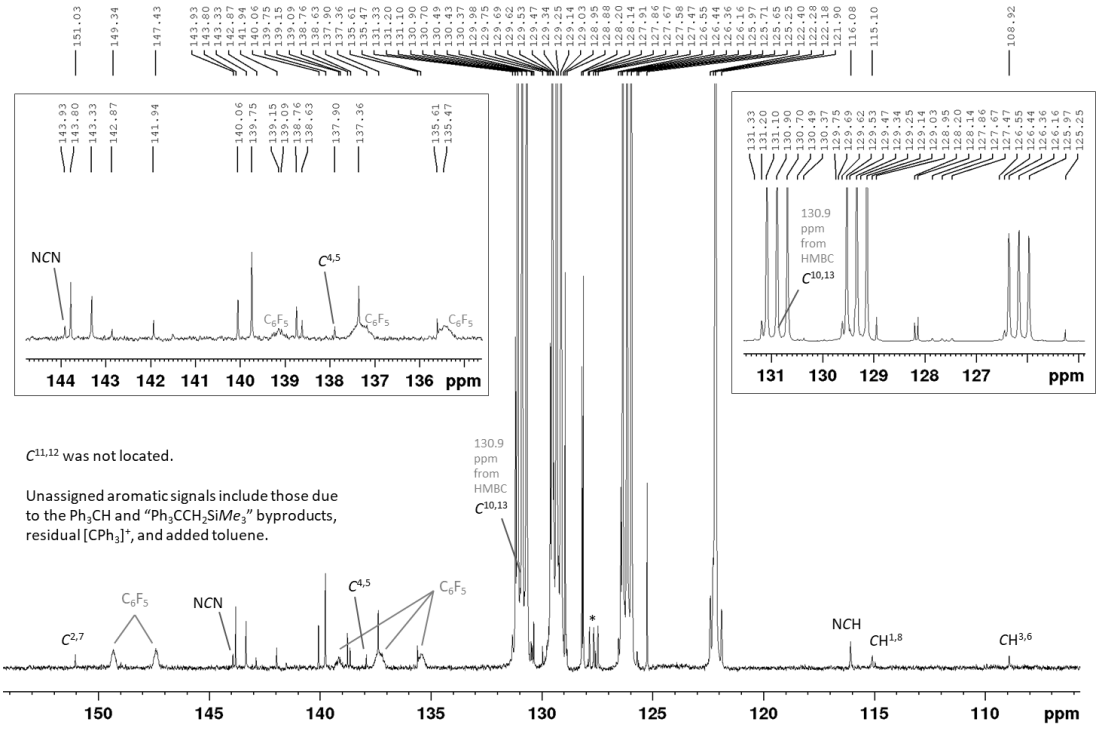

Figure S34. Region of the $^{13}C\{^{1}H\}$ NMR spectrum of in situ generated $[(XII_2)Sc(CH_2SiMe_3)(\eta^x\text{-toluene})_n][B(C_6F_5)_4]_2$ (**5**) in the presence of 5 equivalents of toluene (126 MHz, 298 K, C_6D_5Br).

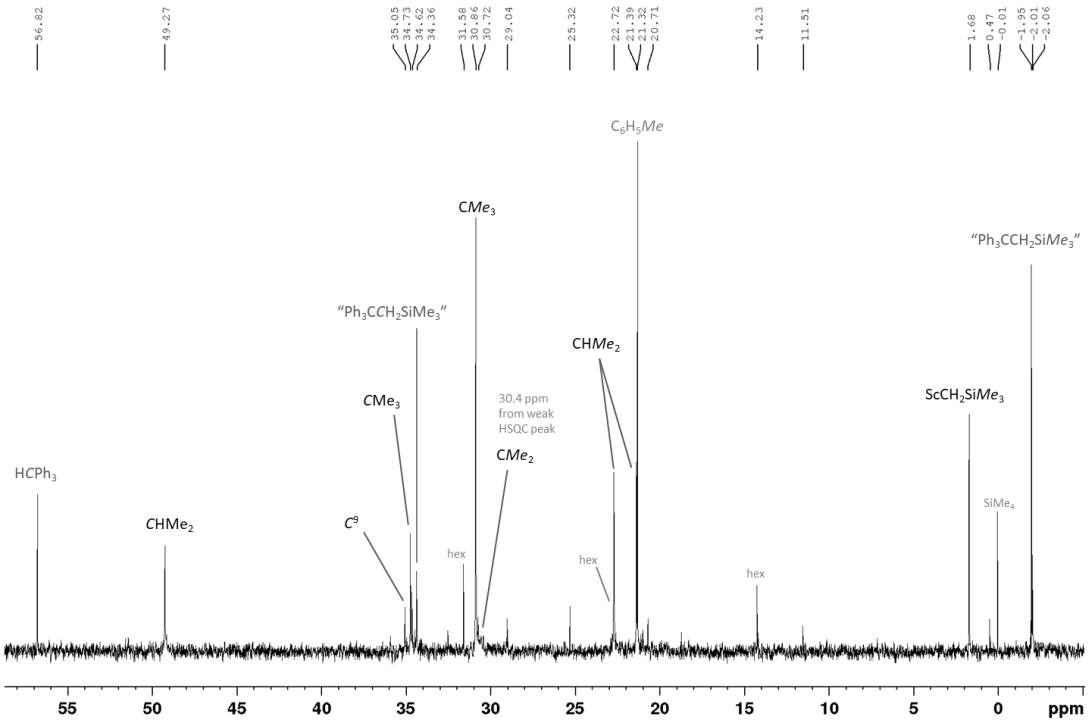

Figure S35. Region of the $^{13}C\{^{1}H\}$ NMR spectrum of in situ generated $[(XII_2)Sc(CH_2SiMe_3)(\eta^x\text{-toluene})_n][B(C_6F_5)_4]_2$ (**5**) in the presence of 5 equivalents of toluene (126 MHz, 298 K, C_6D_5Br).

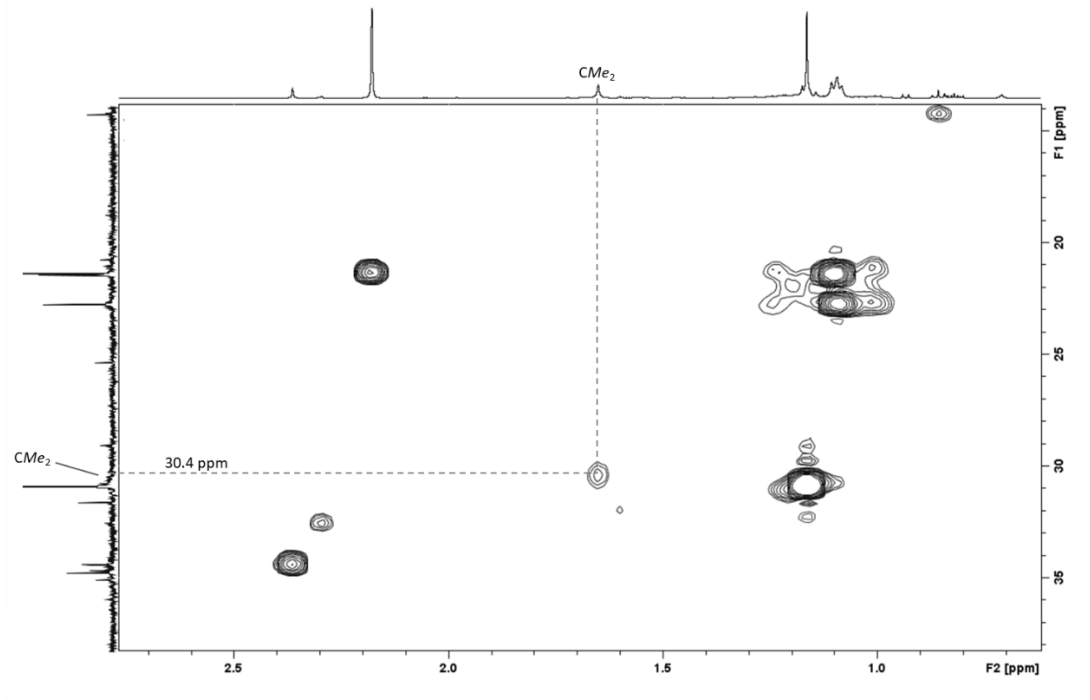

Figure S36. Region of the ^{1}H-^{13}C HSQC NMR spectrum of in situ generated $[(XII_2)Sc(CH_2SiMe_3)(\eta^x\text{-toluene})_n][B(C_6F_5)_4]_2$ (**5**) in the presence of 5 equivalents of toluene (500 MHz ^{1}H, 126 MHz ^{13}C, 298 K, C_6D_5Br). This region enabled location of the ^{13}C NMR C*Me*$_2$ signal. The ^{1}H NMR spectrum is on the horizontal axis. The $^{13}C\{^{1}H\}$ NMR spectrum is on the vertical axis.

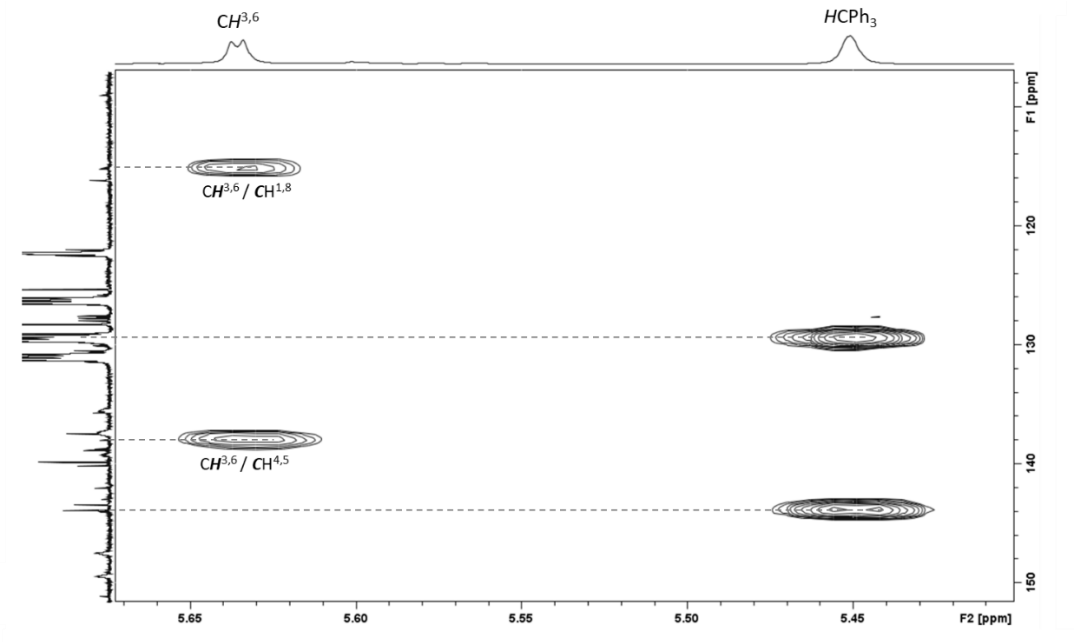

Figure S37. Region of the ^{1}H-^{13}C HMBC NMR spectrum of in situ generated [(XII$_2$)Sc(CH$_2$SiMe$_3$)(η^x-toluene)$_n$][B(C$_6$F$_5$)$_4$]$_2$ (**5**) in the presence of 5 equivalents of toluene (500 MHz ^{1}H, 126 MHz ^{13}C, 298 K, C$_6$D$_5$Br). This region enabled location of the ^{13}C NMR *C*^{4,5} signal. The ^{1}H NMR spectrum is on the horizontal axis. The ^{13}C{^{1}H} NMR spectrum is on the vertical axis.

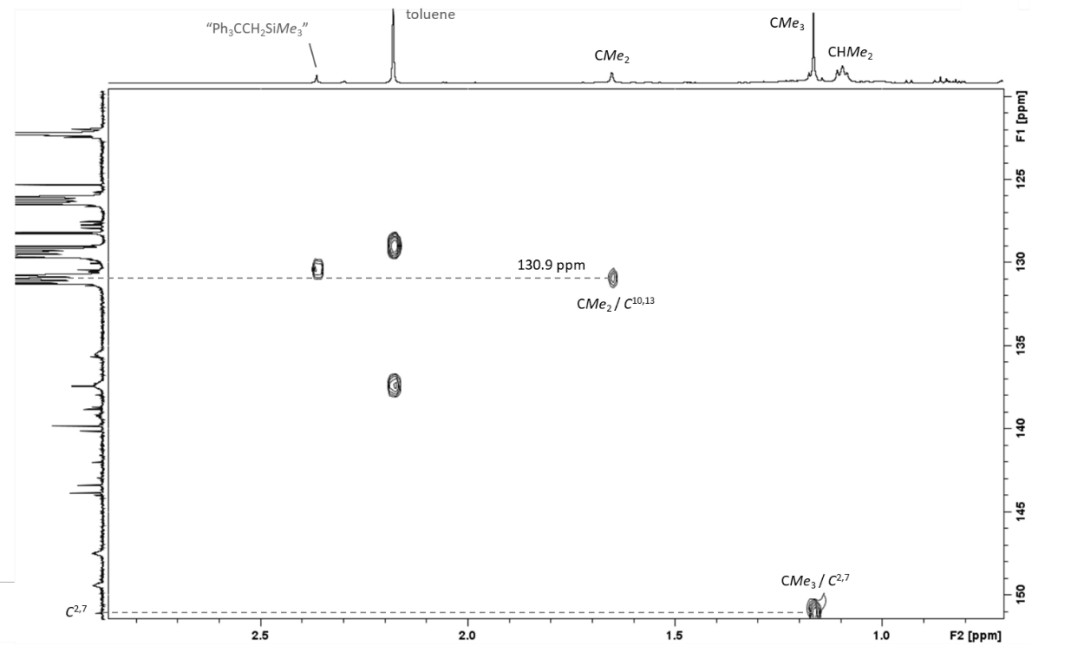

Figure S38. Region of the ^{1}H-^{13}C HMBC NMR spectrum of in situ generated [(XII$_2$)Sc(CH$_2$SiMe$_3$)(η^x-toluene)$_n$][B(C$_6$F$_5$)$_4$]$_2$ (**5**) in the presence of 5 equivalents of toluene (500 MHz ^{1}H, 126 MHz ^{13}C, 298 K, C$_6$D$_5$Br). This region enabled location of the ^{13}C NMR *C*^{10,13} signal. The ^{1}H NMR spectrum is on the horizontal axis. The ^{13}C{^{1}H} NMR spectrum is on the vertical axis.

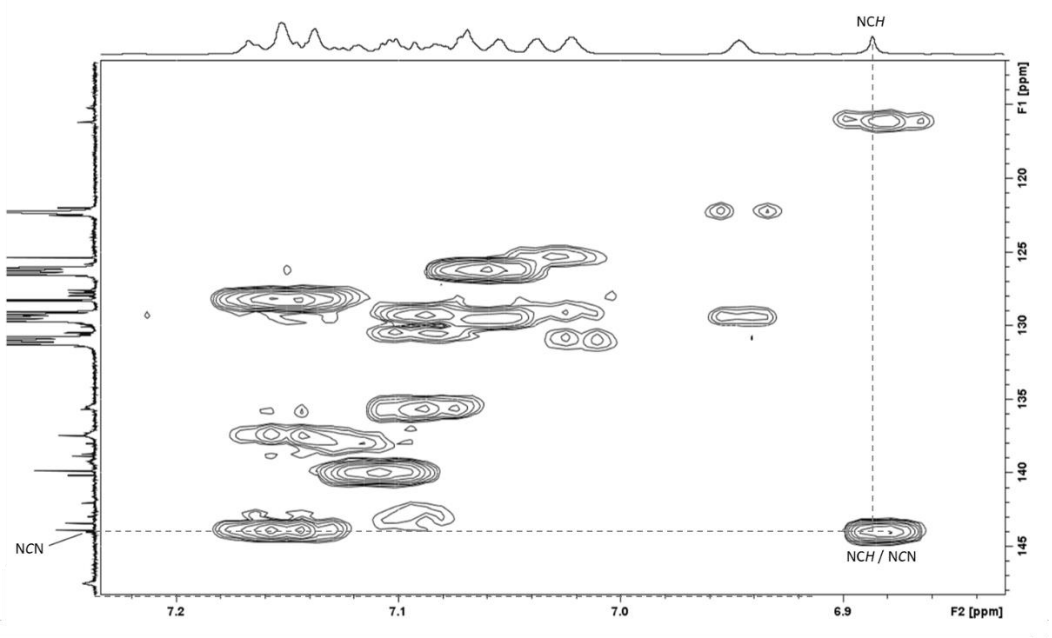

Figure S39. Region of the ^{1}H-^{13}C HMBC NMR spectrum of in situ generated [(XII$_2$)Sc(CH$_2$SiMe$_3$)(η^x-toluene)$_n$][B(C$_6$F$_5$)$_4$]$_2$ (**5**) in the presence of 5 equivalents of toluene (500 MHz ^{1}H, 126 MHz ^{13}C, 298 K, C$_6$D$_5$Br). This region enabled location of the ^{13}C NMR N*C*N signal. The ^{1}H NMR spectrum is on the horizontal axis. The ^{13}C{^{1}H} NMR spectrum is on the vertical axis.

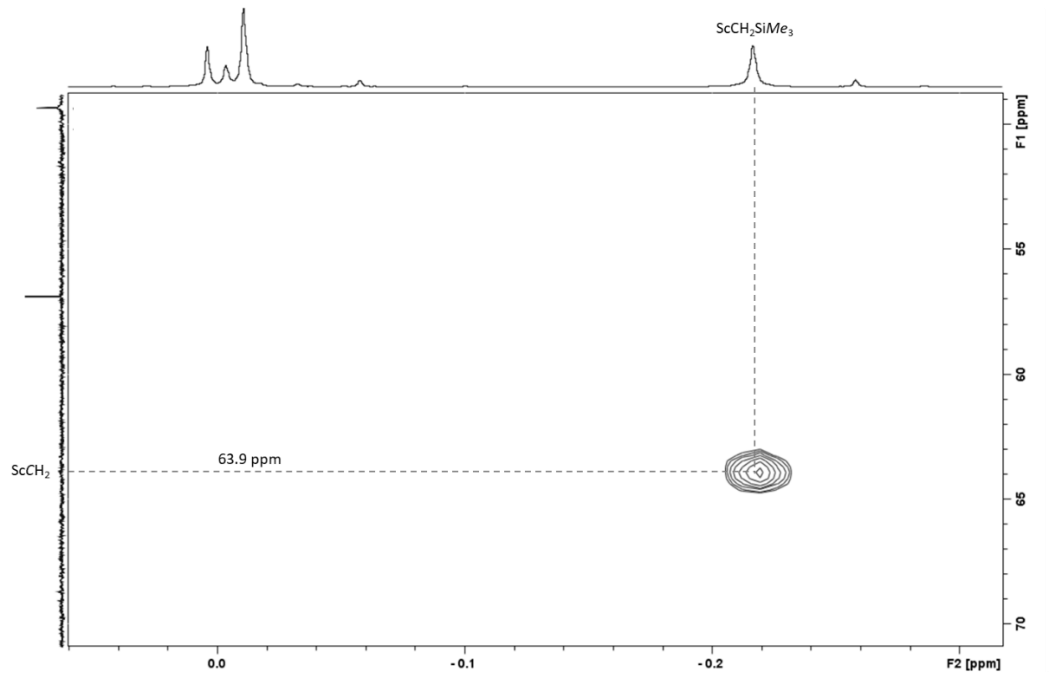

Figure S40. Region of the ^{1}H-^{13}C HMBC NMR spectrum of in situ generated [(XII$_2$)Sc(CH$_2$SiMe$_3$)(η^x-toluene)$_n$][B(C$_6$F$_5$)$_4$]$_2$ (**5**) in the presence of 5 equivalents of toluene (500 MHz ^{1}H, 126 MHz ^{13}C, 298 K, C$_6$D$_5$Br). This region enabled location of the ^{13}C NMR Sc*C*H$_2$ signal. The ^{1}H NMR spectrum is on the horizontal axis. The ^{13}C{^{1}H} NMR spectrum is on the vertical axis.

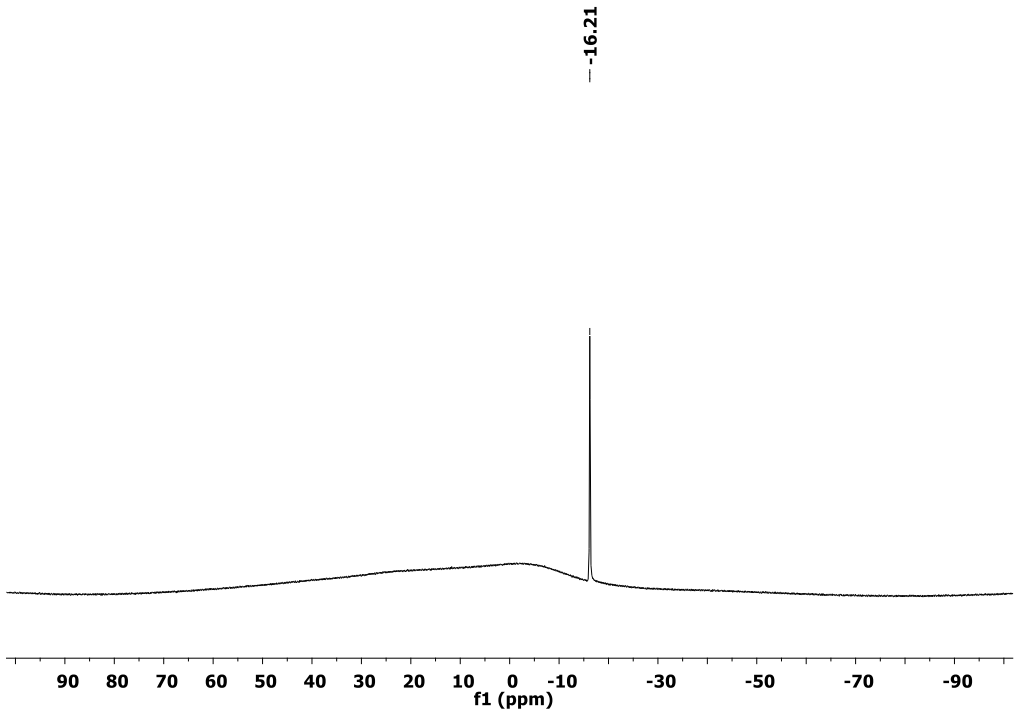

Figure S41. ^{11}B NMR spectrum of in situ generated $[(XII_2)Sc(CH_2SiMe_3)(\eta^x\text{-toluene})_n][B(C_6F_5)_4]_2$ (**5**) in the presence of 5 equivalents of toluene (161 MHz, 298K, C_6D_5Br).

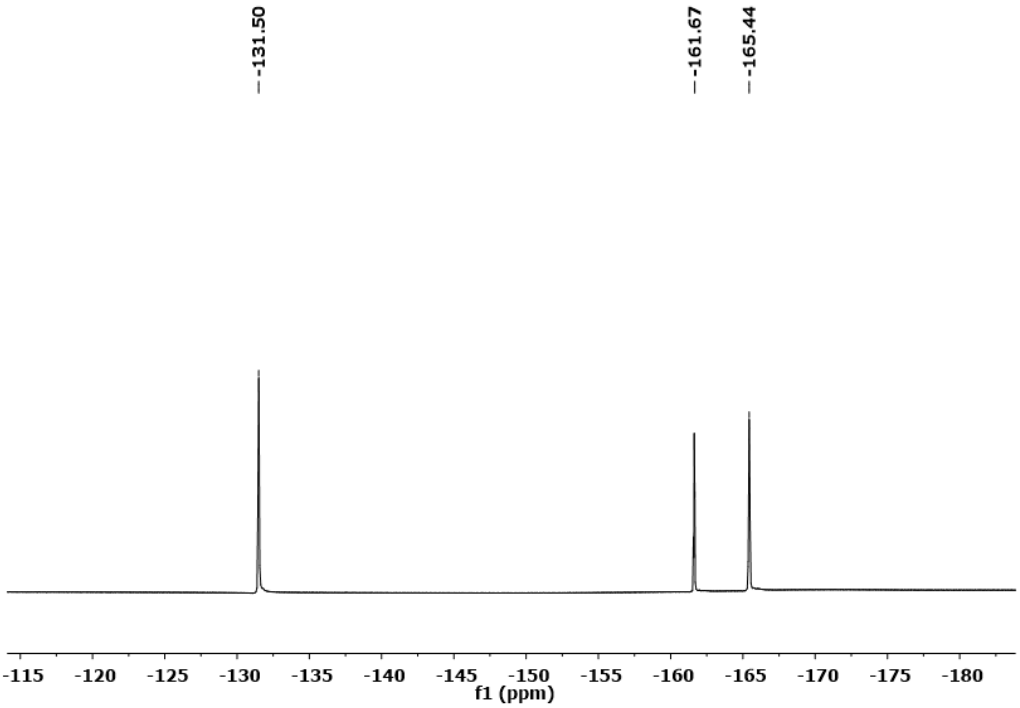

Figure S42. ^{19}F NMR spectrum of in situ generated $[(XII_2)Sc(CH_2SiMe_3)(\eta^x\text{-toluene})_n][B(C_6F_5)_4]_2$ (**5**) in the presence of 5 equivalents of toluene (471 MHz, 298K, C_6D_5Br).

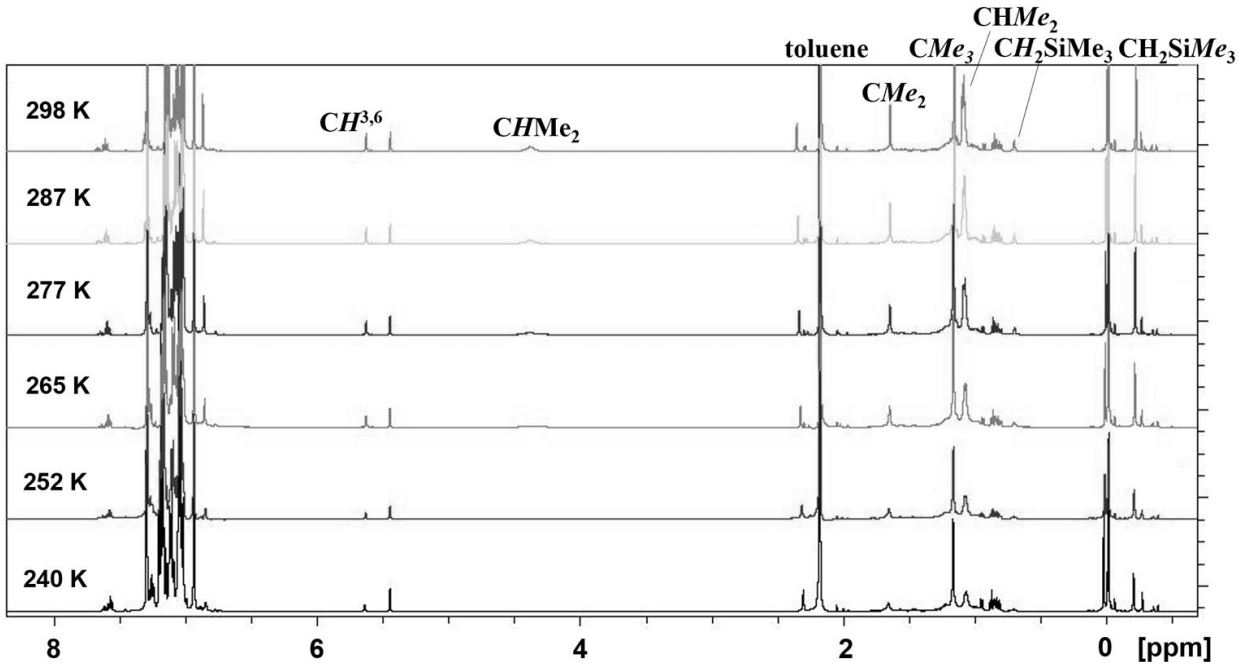

Figure S43. Variable temperature ^{1}H NMR spectra of in situ generated [(XII$_2$)Sc(CH$_2$SiMe$_3$)(η^x-toluene)$_n$][B(C$_6$F$_5$)$_4$]$_2$ (**5**) in the presence of 5 equivalents of toluene (500 MHz, C$_6$D$_5$Br).

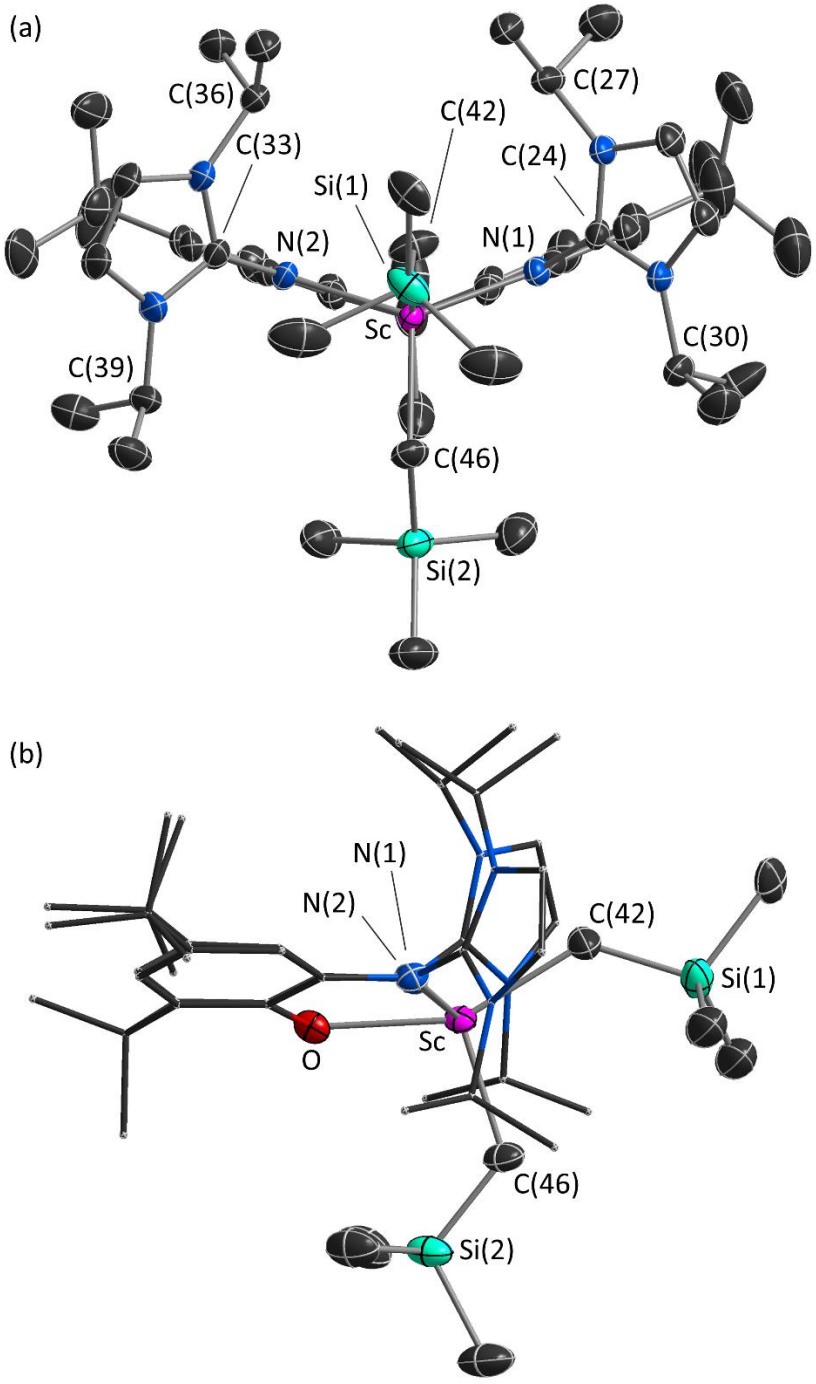

Figure S44. Front and side views of the cationic portion of the X-ray crystal structure of $[(XII_2)Sc(CH_2SiMe_3)_2][B(C_6F_5)_4]\cdot 2PhF$ (**3**·2PhF). Ellipsoids are set to 30% probability and hydrogen atoms are omitted for clarity. One of the CMe_3 groups is disordered, and only one orientation is shown. In view b, all atoms of the XII_2 ligand, except for O, N(1) and N(2) are shown in wireframe. Selected bond lengths (Å) and angles (°): Sc–N(1) 2.190(3), Sc–N(2) 2.190(2), Sc–O 2.282(2), Sc–C(42) 2.228(4), Sc–C(46) 2.211(3), N(1)–C(24) 1.369(4), N(2)–C(33) 1.369(4), C(27)···C(36) 4.598, C(30)···C(39) 8.324, N(1)–Sc–N(2) 126.9(1), O–Sc–C(42) 151.2(1), O–Sc–C(46) 104.8(1), C(42)–Sc–C(46) 104.1(1), Sc–C(42)–Si(1) 130.9(2), Sc–C(46)–Si(2) 123.9(2).

Table S1. Ethylene Polymerization Data for Catalyst **5** (0.2 mM concentration)[a] under 1 atm of Ethylene at room temperature. [§]

Solvent	Polym. Time (min)	Yield (g)	Activity (kg/mol·h·atm)	M_n (kg/mol)	M_w (kg/mol)	M_z (kg/mol)	M_v (kg/mol)	M_p (kg/mol)	M_w/M_n
toluene/ *o*-$C_6H_4F_2$	2	0.239	741	46.77	65.70	98.06	62.76	70.30	1.40
toluene/ *o*-$C_6H_4F_2$	3	0.420	868	79.47	111.88	163.61	106.98	104.82	1.41
toluene/ *o*-$C_6H_4F_2$	5	0.456	565	98.12	202.21	298.45	191.29	205.73	2.06
o-$C_6H_4F_2$	3	0.135	168	132.24	170.55	210.66	165.40	174.86	1.29

[a] The catalyst solution was generated in situ by stirring 15 mg (9.7 µmol) of $[(XII_2)Sc(CH_2SiMe_3)_2][B(C_6F_5)_4]$ (**3**) with 1 equiv. of $[CPh_3][B(C_6F_5)_4]$ (9 mg; 9.8 µmol) in 3 mL of solvent (either a 1:2 mixture of toluene and *o*-$C_6H_4F_2$, or neat *o*-$C_6H_4F_2$) for 2 hours, followed by the addition of an additional 40 mL of solvent (either a 3:1 mixture of toluene and *o*-$C_6H_4F_2$, or neat *o*-$C_6H_4F_2$). Note: The polymerization reactions were exothermic, causing an increase in the solution temperature, despite the room temp. water bath around the flask.

[b] Values from GPC are relative to polyethylene standards.